UNIVERSITÀ DEGLI STUDI DELL'INSUBRIA

DOTTORATO DI RICERCA
Scienze della Vita e Biotecnologie

SCUOLA DI DOTTORATO
UNIVERSITÀ DEGLI STUDI DELL'INSUBRIA

DIPARTIMENTO DI
BIOTECNOLOGIE E SCIENZE DELLA VITA

PhD Course in

LIFE SCIENCES AND BIOTECHNOLOGY

XXXVIII cycle

cAMP-dependent plant stress response

Doctoral Dissertation of:

Eleonora Davide

Supervisor: **Prof. Candida Vannini**

Cosupervisor: **Prof. Chris Gehring**

Tutor: **Dr. Guido Domingo**

Coordinator of the PhD Program: **Prof. Silvia Sacchi**

Academic year 2024/2025

Index

Abstract:

Cyclic monophosphate nucleotides are increasingly recognized as signaling molecules involved in various physiological processes in plants. Among them is cyclic adenosine monophosphate (cAMP), which comes in two isomers: 3',5'-cAMP and 2',3'-cAMP. The former is synthesized by adenylate cyclases (AC), while the latter results from RNA degradation. Using proteomic and electrophysiological approaches in Arabidopsis thaliana, we observed that each isomer exerts distinct effects on the proteome. Specifically, 2',3'-cAMP regulates the transcription systemically. Neither isomer alters ion fluxes under control conditions, but both reduce K^+ efflux and Ca^{2+} influx under oxidative stress. CNGC2 and CNGC18 channels interact exclusively with 3',5'-cAMP, indicating isomer-specific gating. Additionally, 3',5'-cAMP is involved in the plant heat stress response (HSR), regulating protective cellular networks. Due to climate change, the frequency and intensity of heatwaves have increased, negatively affecting plant growth and yield. This thesis investigates the role of intracellular 3',5'-cAMP in HSR in Arabidopsis, using transgenic lines (cAS1 and cAS3) that express a "cAMP sponge" construct capable of selectively sequestering 3',5'-cAMP. Physiological, biochemical, and transcriptomic analyses clarify the contribution of this isomer to plant heat stress resilience.

Abbreviations

2',3'-cAMP: cyclic adenosine 2'3'-monophosphate
3',5'-cAMP: cyclic adenosine 3'5'-monophosphate
ABA: abscisic acid
AC: Adenylate cyclase
AFBs: Auxin-Signaling F-Box proteins
APX2: Ascorbate peroxidase 2
ASC: Ascorbate
ASC: ascorbate
BSA: bovine serum albumin
BSM: basic salt medium
CaMBD: Calmodulin binding domain
cAMP (in chapter 4): refers only to cyclic adenosine 3'5'-monophosphate
cAMP: cyclic adenosine monophosphate
CAT: catalase
CBF1: C-repeat Binding Factor 1
cGMP: cyclic guanosine 3'5'-monophosphate
CLPB3: Casein Lytic Proteinase B3
CMTA3: Calmodulin-binding Transcription Activator 3
CNGCs: cyclic nucleotide-gated channels
cNMPs: cyclic nucleotide monophosphates
COLD6: Chilling-tolerance divergence 6
DAB: 3,3'-diaminobenzidine
DAPs: differentially abundant proteins
DEGs: differentially expressed genes
DHA: dehydroascorbate
DOF5.4: DNA-binding with One Finger 5.4
DREB1A: Dehydration-Responsive Element-Binding protein 1A
DTNB: 5,5′-dithiobis(2-nitrobenzoic acid)
DTT: dithiothreitol
EDTA: Ethylenediaminetetraacetic acid
EPACs: Exchange Proteins directly Activated by cAMP
ERF: Ethylene Response Factor
FASP: Filter Aided Sample Preparation
FDR: false discovery rate
GBF1: G-box Binding Factor 1
GO: gene ontology

GR: glutathione reductase

GSH: glutathione

GUN5: Genomes Uncoupled 5

HEPES: 4-(2-hydroxyethyl)-1-piperazineethanesulfonic acid

HPLC: high-performance liquid chromatography

HS: heat stress

HSF7B: heat shock factor 7B

HSFA2: heat shock factor A2

HSFA8: Heat Shock Factor A8

HSFs: Heat Shock Factors

HSP21: Heat Shock Protein 21

HSP90: heat shock protein 90

HSPs: Heat Shock Proteins

HSR: heat shock response

IBMX: 3-isobutyl-1-methylxanthine

KEGG: Kyoto Encyclopedia of Genes and Genomes

LARP: La-Related protein

LHCB: Light-Harvesting Chlorophyll a/b-Binding Protein 1.1

LPB3: Casein Lytic Proteinase B3

MIFE ®: non-invasive microelectrode ion flux estimation

MS: Murashige and Skoog medium

NADPH: nicotinamide adenine dinucleotide phosphate

NBT: nitroblue tetrazolium

NCED3: chloroplastic protein 9-cis-epoxycarotenoid dioxygenase 3

NEM: N-ethylmaleimide

NO: nitric oxide

OSM1: osmotin-like 1

PBC: phosphate binding cassette

PBS: Phosphate-Buffered Saline

PCA: Principal Component Analysis

PDEs: phosphodiesterases

PKA: protein kinase A

PPI: protein-protein interaction

PSBO: Photosystem II Oxygen-Evolving Enhancer Protein

RBOHD: Respiratory Burst Oxidase Homolog D

RBOHs: respiratory burst oxidase homolog proteins

ROS: reactive oxygen species

SOD: superoxide dismutase

STRING: Search Tool for the Retrieval of Interacting Genes/Proteins

STZ: Salt Tolerance Zinc Finger

TBE: Tris-Borate-EDTA

TCA: trichloroacetic acid

TDTHub: TFBS-Discovery Tool Hub

TEM: Transmission electron microscopy

TEVC: two-electrode voltage clamp

TF: transcription factor

TFBS: transcription factor binding sites

TIR1: Transport Inhibitor Response 1

TMM: Trimmed Mean of M-values

WRKYs: WRKY DNA-binding protein

WT: wild-type

XTT: [2,3-bis(2-methoxy-4-nitro-5-sulfophenyl)-2H-tetrazolium-5-carboxanilide]

Chapter 1: General introduction

1.1 The history and controversy of cAMP in plants

All living organisms rely on highly complex signalling networks that enable the rapid perception of environmental changes and the integration of this information into adaptive responses. This is particularly true for plants, which are sessile organisms. These signaling processes involve receptors, transducers, and downstream effectors, but critically depend on second messengers, small, diffusible molecules that relay signals from activated receptors to intracellular targets. Well-characterized second messengers include Ca^{2+}, reactive oxygen species (ROS), cyclic nucleotide monophosphates (cNMPs), inositol phosphates, and nitric oxide (NO).

Among these, the cNMPs, namely cyclic adenosine 3'5'-monophosphate (cAMP) and cyclic guanosine 3'5'-monophosphate (cGMP), represent chemical signals controlling a vast number of processes in all biological systems [1]. However, in higher plants, the existence and physiological functions of these 3',5'-cNMPs have required a long time to be accepted since their contents were significantly lower than those found in animals and were hardly detectable because cellular levels were below the detection limits of available analytical methods [2].

In particular, he role of 3',5'-cAMP has been well established as a second messenger in mammalian cells since 1957, when it was first reported by Rall and Sutherland (1958) [3]. Shortly thereafter, its role as a signaling molecule was also discovered in bacteria [4] and yeast [5]. In contrast, its presence and function in plants have long been debated [6, 7]. This controversy largely stems from the technical challenges associated with detecting 3',5'-cAMP in plant tissues, where its concentration is approximately an order of magnitude lower than in animal systems, making it difficult to detect with available analytical methods. Furthermore, the presence of interfering plant compounds has complicated its quantification. Nevertheless, a potential role for 3',5'-cAMP in plant systems had already been proposed in the early 1970s [8]. A significant turning point occurred in 1994, when Li and colleagues provided the first functional evidence that 3',5'-cAMP regulates ion channel activity in higher plant cells, thereby demonstrating a physiological role in ion transport across the plasma membrane [9].

Further challenges arose from the apparent absence of canonical plant homologs of two major animal 3', 5'-cAMP effectors: Protein Kinase A (PKA), an enzyme activated by 3',5'-cAMP that phosphorylates diverse targets involved in growth, metabolism, and stress responses, and the Exchange Proteins directly Activated by cAMP (EPACs), which represent central effectors of cAMP signalling in animal systems [10]. Similarly, adenylate cyclases, enzymes responsible for the production of 3',5'-cAMP from ATP, and phosphodiesterases, which regulate its levels, had not been fully characterized in plants [2].

Continuous methodological advances have gradually resolved much of the controversy. Improvements in analytical chemistry, particularly the introduction of high-performance liquid chromatography (HPLC) and electrospray ionisation mass spectrometry, dramatically increased sensitivity (to as low as 25 femtomoles for cyclic nucleotides). These improvements have permitted reliable detection and quantification of 3',5'-cAMP in plant tissues that typically maintain nanomolar concentrations, based on fresh weight [2]. Particularly, 3',5'-cAMP is supposed to work in micro-environments with levels that are usually < 20 pmol/g fresh weight within plant tissues [11].

1.2 Adenylate Cyclases and 3',5'-cAMP production in plants

Adenylate cyclases (ACs) are cytoplasmic or plasma-membrane-associated enzymes that catalyse the conversion of ATP to 3',5'-cAMP and pyrophosphate.significant step forward was in 2001 when the first plant-soluble AC (PSiP), involved in pollen tube reorientation, was identified in *Zea mays* and in *Agapanthus umbellatus* [12]. The use of a 14-amino-acid search motif, resulting from the catalytic centers of annotated and experimentally confirmed ACs, has permitted, in the last decade, the identification of many new ACs in higher plants [2, 13, 14]. To date, several proteins with AC activity have been reported in nine species of higher plants (*Arabidopsis thaliana, Brachypodium distachyon*, *Glycine max*,

Hippeastrum × *hybridum*, *Malus domestica*, *Nicotiana benthamiana*, *Pyrus bretschneider*, *Zea mays*, *Ziziphus jujuba*) and one in the basal plant liverwort (*Marchantia polymorpha*) [15].

In many identified ACs, the catalytic centers are embedded within multidomain proteins that contain additional domains with well-defined primary functions. These proteins, commonly referred to as moonlighting proteins, exhibit diverse architectures in which AC activity is confined to relatively small regions of otherwise multifunctional proteins [16, 17]. Their enzymatic activity is generally lower than that of canonical stand-alone ACs, and they are thought to contribute to fine-tuned regulatory processes. Accordingly, such proteins are termed crypto-ACs [16, 17]. Notably, the coexistence of multiple functional domains within a single protein points to complex regulatory mechanisms, although it remains unclear whether these domains operate concurrently or modulate one another through intramolecular interactions [14]. AtKUP7 and AtKUP5 are two examples of moonlighting/cryptic ACs recognised in *A. thaliana*, involved in K^+ uptake and translocation in roots. AtKUP5 transports K^+ into the cell and generates 3',5'-cAMP through its cytosolic N-terminal AC domain [18].

1.3 Regulation of 3', 5'-cAMP levels by phosphodiesterases

Given that cAMP functions as a signaling molecule, its degradation is just as crucial as its synthesis for maintaining the transient and dynamic regulation of intracellular 3',5'-cAMP levels, which are essential for many physiological and developmental processes [1, 19]. However, this aspect remains largely unexplored compared to ACs. The "off" signal is mediated by phosphodiesterases (PDEs). Based on sequence analysis and the structural properties of canonical PDE catalytic centers, a consensus sequence search motif has been developed and used to identify candidate PDEs [19].

In *Arabidopsis thaliana*, more than 20 proteins have been identified with a twin AC–PDE architecture, characterized by an N-terminal AC motif and a C-terminal PDE motif, reflecting a sophisticated mechanism of cAMP-dependent signaling [19]. A notable example is the K^+ channel AtKUP5, whose C-terminal PDE domain is activated by Ca^{2+} influx, itself enhanced by 3',5'-cAMP, thereby enabling tight control of 3',5'-cAMP turnover and fine regulation of K^+ homeostasis (Fig. 1).

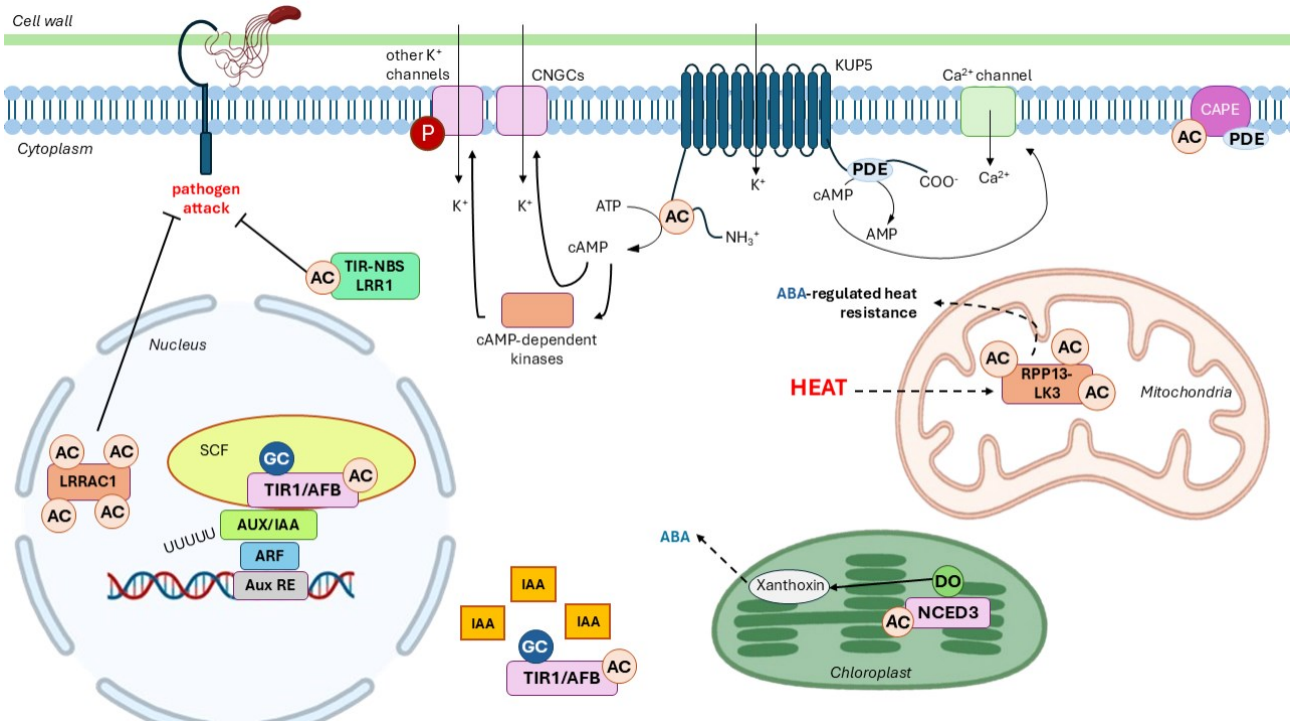

Figure 1. Schematic representation of different ACs and PDE activity. ABA, Abscisic acid; AC, adenylate; AFB, auxin-signaling F-box; ARFs, auxin response factors; Aux/IAA, transcriptional repressor Auxin/Indole-2-Acetic Acid; 3',5'- cAMP, cyclic adenosine 3'5'-monophosphate; CAPE, combined AC with PDE; DO, dioxygenase; GC, guanylate cyclase; IAA, indole-2-acetic acid; KUP, K1-uptake permease; LRR, leucine-rich repeat; NCED3, 9- cis -epoxycarotenoid dioxygenase; PDE, phosphodiesterase; PPR, pentatricopeptide repeat; RPP13-LK3, RPP13-like protein 3; TIR-NBSLRR, toll interleukin-like receptor-nucleotide-binding siteleucine-rich repeat; TIR1, transport inhibitor response 1. Created in https://BioRender.com. Figure adapted from Fortunato et al., 2025 [20]

1.4 Physiological roles of 3'.5'-cAMP in plants

Significant advances in plant biology research, complemented by omics and biochemical studies, have led to the characterization of the 3',5'-cAMP as a key signaling molecule in plants as well. It is critically involved in both plant development and environmental stress response, contributing to several signaling pathways crucial for processes such as stomatal movement, through Ca^{2+} and K^{+} flux regulation [21] antagonising the effect of ABA [22]; ion homeostasis, mainly through the regulation of membrane-localised ion channels; pollen tube orientation and growth, through the regulation of Ca^{2+} fluxes and choline acetyltransferase activity; cell cycle progression, where 3',5'-cAMP peaks were observed during the S and G1 phases; seeds germination and responses to both biotic and abiotic environmental stresses [21].

Recent studies connect 3',5'-cAMP with auxin signaling, highlighting its involvement in plant development. The auxin receptors Transport Inhibitor Response 1 (TIR1) and Auxin-Signaling F-Box proteins (AFBs), F-box subunits of the SCF ubiquitin ligase complexes, harbor a conserved AC motif. Phylogenetic studies have also revealed that the AC motif is conserved in *Physcomitrella patens*, pointing to an ancient evolutionary origin. In *Arabidopsis thaliana*, TIR1, AFB1, and AFB5 can generate cAMP, and this activity is further stimulated by auxin and Aux/IAA proteins [23]. Mutations disrupting the AC motif abolish cAMP production and interfere with the long-term effects of auxin on root growth and gravitropism, underscoring the requirement of adenylate cyclase activity for auxin-mediated transcriptional regulation. More recently, it has been shown that TIR1/AFB receptors also display guanylate cyclase activity, producing cGMP upon auxin stimulation. Unlike cAMP, auxin-triggered cGMP synthesis is involved in rapid cellular responses [24].

Several literature data suggest the involvement of 3',5'-cAMP in biotic and abiotic stresses. Plants are continuously exposed to a variety of invading microorganisms, including viruses, bacteria, and fungi, which can release elicitors into plant cells. These elicitors can trigger the activation of adenylyl cyclases (ACs), leading to an increase in intracellular cAMP levels. Elevated cAMP may, in turn, activate cyclic nucleotide-gated channels (CNGCs), promoting cytosolic Ca^{2+} influx, or stimulate the production of ROS through the activation of enzymes such as NADPH oxidases [25].

The adaptation of plants to external stimuli such as heat, drought, or salinity is intricately linked to the modulation of ion channels and the control of ion fluxes. In this context, 3',5'-cAMP plays a significant role in mediating responses to various abiotic stresses. For instance, under salinity stress, cAMP is involved in the limitation of Na^+ influx through voltage-independent channels and CNGCs. In conditions of aluminium toxicity, cAMP facilitates K^+ currents that permit malate outflow through cation channels. During K^+ deficiency, cAMP contributes to K^+ homeostasis regulation via channels such as AtKUP5 and AtKUP7, as well as CNGCs [21].

In drought conditions, cAMP contributes to the synthesis of protective polypeptides through ABA signaling. Strong evidence of the role of cAMP in abiotic stress is the link between 3',5'cAMP and the stress hormone ABA. In *Arabidopsis thaliana*, the chloroplastic protein 9-cis-epoxycarotenoid dioxygenase 3 (NCED3, At3g14440), essential for ABA biosynthesis, contains a functional AC center. NCED3 synthesizes 3',5'-cAMP in vitro, with activity enhanced by Ca^{2+}, and structural analyses suggest that its dioxygenase and AC functions may operate independently [17]. Both ABA and cAMP regulate overlapping processes, including osmosis, light and salt stress responses, and energy metabolism [26–28], positioning AtNCED3 as a key node in ABA–3',5'cAMP crosstalk.

A similar link has been reported in maize under heat stress, where the protein ZmRPP13-LK3 and ZmPSiP, harboring conserved AC motifs, show inducible AC activity [12, 29]. Their expression and cAMP content were increased by heat stress in an ABA-dependent way in maize roots. Moreover, treatment with a cAMP analogue enhanced heat-shock protein expression and reduced oxidative damage, supporting a role for 3',5'-cAMP in ABA-dependent heat stress responses [30].

Numerous studies emphasize the progressively pivotal role of 3'-5' cAMP in the signaling pathways activated by plants in heat stress response (HSR), with cAMP implicated in multi-level regulatory networks that prevent cell damage and maintain cellular homeostasis [21]. 3',5'-cAMP is thought to mediate plant adaptation to heat stress by regulating ion fluxes, mainly through CNGCs [21, 31]. Heat-induced accumulation of 3',5'-cAMP has been shown to activate the CNGC6 in Arabidopsis thaliana, triggering a Ca^{2+} influx into the cell. This rise in cytosolic Ca^{2+} contributes to the induction of Heat Shock Factors (HSFs) and the consequent Heat Shock Protein (HSP) gene expression, thereby promoting the acquisition of thermotolerance [32, 33].

Another consequence of high temperature is the overproduction of ROS, such as H_2O_2. The respiratory burst oxidase homolog proteins (RBOHs) are essential for generating ROS in the apoplast space under stress [34]. Some studies suggest a complex relationship between 3'5'-cAMP and RBOHs expression in plants and animals [30, 35–37]. ROS species can act as signaling molecules, thanks to a fine balance between production and scavenging, which regulates their levels within cells. As molecular signals, ROS induce changes in cellular metabolism, leading to adaptive responses or triggering programmed cell death (PCD) [38–40]. The application of 3',5'-cAMP increased the activity of antioxidant enzymes such as ascorbate peroxidases and superoxide dismutase under heat stress, while the failure in 3',5'-cAMP elevation in tobacco BY2 cells decreases the accumulation of proteins involved in ROS detoxification and redox homeostasis [37].

1.5 Emergence and Biological Relevance of the 2',3'-cAMP isomer in plants

In recent years, questions have emerged regarding the specific roles of the newly recognized 2′,3′-cNMP isomers, particularly regarding 2′,3′-cAMP. This molecule, which differs from 3',5'-cAMP in the position of the phosphate linkage (Fig.2) was first detected in biological material relatively recently [41]. 2',3'-

cAMP arises as an RNA degradation intermediate generated by the activity of ribonucleases. In response to pathogens and abiotic stresses, RNA is released and can be converted by synthetases into 2′,3′-cAMP/cGMP. This mechanism may explain the elevated cellular levels of 2′,3′-cAMP observed under wounding stress, heat, and darkness [8, 44, 45]. More recently, it was shown in *Nicotiana benthamiana* that the Toll/interleukin-1 receptor (TIR) protein is capable of synthesizing 2',3-cAMP through RNA or double-stranded DNA hydrolysis. TIR domains have bifunctional activity as an NADase or 2',3'-cAMP synthetase, and this is required for TIR-mediated cell death [8].

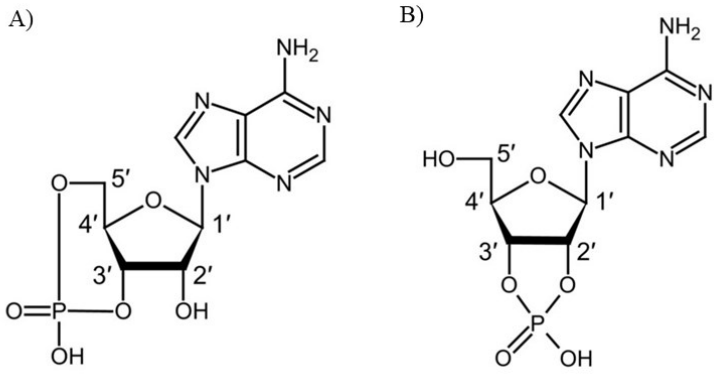

Figure 2. cAMP molecules, A) 3',5'-cAMP and B) 2',3'-cAMP.

However, higher plants possess PDEs dedicated to the inactivation of 2',3'-cAMP. Among them, NUDT7 has been identified as a negative regulator of TIR–NLR signaling: its overexpression in *N. benthamiana* suppresses TIR1-dependent cell death, whereas *Atnudt7* mutants accumulate higher levels of 2′,3′-cAMP, suggesting its role in hydrolyzing this molecule during immune responses [8]. Interestingly, a PDE capable of hydrolyzing both 2',3'-cAMP and 3',5'-cAMP was identified in *Pisum sativum* seedlings [42]. This enzyme catalyzes the hydrolysis of 2',3'-cAMP to yield 2'-AMP and 3'-AMP [43], whereas 3',5'-cAMP is hydrolyzed into a mixture of 3'-AMP and 5'-AMP [1]. The presence of dual-specificity phosphodiesterases (PDEs) underscores the biochemical interplay and potential cross-regulation between 3′,5′-cAMP and 2′,3′-cAMP isomers in plant signaling pathways.

Together, these findings support the involvement of this isomer in plant stress responses [43–45]. Although studies on responses to the 2′,3′ -cAMP are still limited, available evidence suggests that its action occurs at the systems level. In *A. thaliana*, 2',3'-cAMP treatment induces extensive changes in the transcriptome, proteome, and metabolome, notably affecting pathways linked to stress responses [46]. Moreover, the binding of 2',3'-cAMP to the RNA-binding protein Rbp47b promotes the stress granule (SG) assembly. SGs are large ribonucleoprotein complexes that selectively store and protect mRNAs, thereby regulating the stress translatome [46]. More recently, it has been demonstrated in rice that the cold sensor complex of Chilling-tolerance divergence 6 (COLD6) and osmotin-like 1 (OSM1) triggers 2',3'-cAMP production under cold stress. Exogenous application of 2',3'-cAMP was further shown to induce *DREB1C* expression and significantly enhance chilling tolerance [47].

Overall, these findings suggest a functional distinction: 3′,5′-cAMP acts at low concentrations in localized microenvironments as a molecular tuner of plant development and defence, whereas 2′,3′-cAMP functions at higher concentrations at the systems level in stress responses.

A schematic summary about the main differences between 3',5'-cAMP and 2',3'-cAMP is presented in Fig.3.

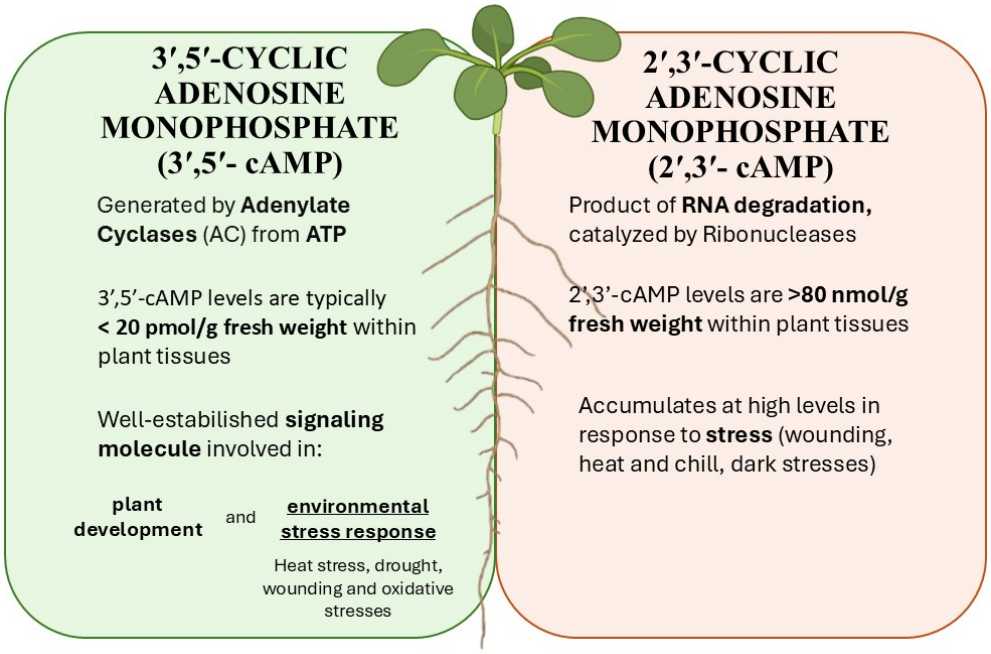

Figure 3. Schematic comparison between 3',5'-cAMP and 2',3'-cAMP in plants.

Chapter 2: Research aims

cAMPs are increasingly recognized as regulators of plant cell signaling and responses. Despite this, the precise roles of individual isomers and the specificity of their actions remain largely unresolved. This PhD research is therefore focused on addressing these gaps through two main objectives:

Aim 1: Functional signatures of two cAMP isomers

The first aim is to determine whether distinct functional signatures delineate 3′,5′-cAMP from its 2′,3′ positional isomers. To this end, a proteomic analysis was conducted following treatment with both isoforms, in order to identify proteins whose expression patterns differed between the two conditions. In addition, non-invasive microelectrode ion flux estimation (MIFE ®) and two-electrode voltage clamp techniques were performed to determine whether the two isomers, both implicated in biotic and abiotic stress responses, share common molecular targets. the MIFE technique was used to measure net cation fluxes under oxidative stress, allowing a comparison between the protective functions of 3',5'-cAMP and the less characterized 2',3'-cAMP. Furthermore, to gain deeper insights into the interaction between cAMPs and CNGCs, CNGC2 and CNGC18, known for their well-established interaction with 3',5'-cAMP, were used as reference targets for our investigation.

Aim 2: Role of 3′,5′-cAMP in basal thermotolerance

Basal thermotolerance is the inherent ability of plants to survive and recover from an episode of heat shock without prior acclimation. This trait is crucial for understanding how plants naturally cope with heat stress, a topic of increasing importance in the context of global climate change. Although 3′,5′-cAMP is recognized as a key signaling molecule in heat stress response, the 3′,5′-cAMP-dependent pathways under HS remain largely unresolved. To address this, *Arabidopsis thaliana* plants overexpressing the "cAMP-sponge" (cAS plants) were used [7]. The "cAMP sponge", consisting of two high-affinity cAMP-binding domains from the human PKA Iβ regulatory subunit, specifically sequesters the active pool of 3',5'-cAMP, thereby reducing its intracellular levels [48].

This genetic tool allows overcoming the limitations associated with a pharmacological approach, which does not consider the importance of physiological concentrations and endogenous fluctuations of 3',5'-cAMP. Two-week-old seedlings were grown under control conditions (22 °C) or subjected to HS (2 h at 45 °C) followed by a short (3h) or long (48h) recovery at 22 °C. Plant performance was assessed by measuring photosynthetic pigments, growth, plastid ultrastructure, and redox homeostasis in both genotypes. Finally, a large-scale comparative transcriptomic analysis was performed on control and HS-treated seedlings to identify specific cAMP-dependent, HS-responsive genes, providing further mechanistic insights into the role of 3′,5′-cAMP in plant basal thermotolerance.

Chapter 3:

Submitted August 2025 – Journal of Experimental Botany

Delineating plant responses to the 3',5'- and 2',3'-cAMP isomers

Eleonora Davide[1], Guido Domingo[1], Angela Di Iacovo[1], Milena Marsoni[1], Ping Yun[3], Chris Gehring[2§], Elena Bossi[1], Sergey Shabala[3,4], Marcella Bracale[1], Candida Vannini[1§]

[1] Department of Biotechnology and Life Science, University of Insubria, 21100 Varese, Italy

[2] Department of Chemistry, Biology and Biotechnology, University of Perugia, 06121 Perugia, Italy

[3] School of Biological Sciences, The University of Western Australia, Perth, WA 6009, Australia

[4] International Research Centre for Environmental Membrane Biology, Foshan University, Foshan, China

§ corresponding authors

edavide@uninsubria.it

g.domingo@uninsubria.it

angela.diiacovo@uninsubria.it

milena.marsoni@uninsubria.it

ping.yun@uwa.edu.au

christophandreas.gehring@unipg.it

Elena.Bossi@uninsubria.it

sergey.shabala@uwa.edu.au

marcella.bracale@uninsubria.it

candida.vannini@uninsubria.it

Running title: Responses to cAMP isomers in plants

Highlights

Distinct Arabidopsis responses to 3’,5’- and 2’,3’-cAMP uncover isomer-specific molecular targets and physiological effects in cyclic nucleotide signaling.

Abstract

Similar to animals, both the 3',5- and the 2,'3'-cAMP isomers are present in plants. The former is the enzymatic product of adenylate cyclases (ACs), the latter is an RNA degradation product. While there is increasing evidence that both isomers can elicit or modulate a broad range of physiological responses, the question of isomer specificity of responses has remained largely unresolved. To delineate isomer-specific responses in *Arabidopsis thaliana* at the systems level, we have combined a comparative proteomics and electrophysiological approaches. Both isomers cause distinct systemic effects on the proteome, with the 2',3' isomer notably affecting systems-level functions like transcriptional regulation. None of the isomers affects net ion fluxes in the root under control conditions, but both were able to attenuate the magnitude of oxidative stress-induced K^+ net loss and Ca^{2+} uptake by 2-fold. Isomer-specific responses of single molecular targets were assessed in the cyclic nucleotide-gated channels 2 and 18 (CNGC2 and CNGC18). Both channels are gated by the 3',5'-cAMP isomer only, suggesting that the gating is isomer-specific and this implies that gating *in vivo* depends on catalytically active ACs.

Keywords

2’,3’-cAMP, 3’,5’-cAMP, Arabidopsis *thaliana*, proteomics, CNGC2 and CNGC18

Introduction

Cyclic nucleotide monophosphates (cNMPs) are increasingly recognised as key signalling molecules that directly or indirectly elicit or modify many diverse physiological processes in plants. Among these cNMPs, the cyclic adenosine monophosphate (cAMP) comes in two isomers, 3’,5’-cAMP and 2’,3’-cAMP. The first, 3',5’-cAMP, is the catalytic product of adenylate cyclases (ACs) that convert ATP into cAMP and pyrophosphate. The second one is the positional isomer 2’,3’-cAMP and is an RNA degradation product catalysed by ribonucleases.

Past reports of plant responses to exogenously applied cAMP largely ignored the specificity of the positional isomer used. Hence, uncertainty prevails in reports that describe cAMP-dependent calcium signaling [1, 2], potassium channel activation [3], self-incompatibility responses [4], sodium uptake [5] and the roles in phytoalexin accumulation [6], phenylpropanoid pathway regulation [7], and root heat tolerance [8].

Recent exclusive studies of 2’,3’-cAMP in plants recognised the 2',3' isomer of cAMP as a stress-associated signalling molecule. Functional studies have shown that 2’,3’-cAMP accumulates in response to wounding, heat stress, darkness, and cold [9–11]. In *A. thaliana*, 2’,3’-cAMP treatment can trigger extensive changes in the transcriptome, proteome, and metabolome, notably affecting pathways linked to stress responses [12]. More recently, it has been demonstrated in rice that exogenous application of 2’,3’-cAMP induces *DREB1C* expression and significantly enhances chilling tolerance. Incidentally, this effect was not observed in

response to 3',5'-cAMP [11]. However, to the best of our knowledge, there are currently no reports of effects elicited by 2',3'-cAMP on the ion transport and, in particular, on the gating of cyclic nucleotide-gated channels (CNGCs). Here, we set out to compare the effects of 3′,5′-cAMP and 2′,3′-cAMP in *A. thaliana*, with the aim of assigning specific response signatures elicited by the two isomers. We performed a quantitative proteomics analysis on seedlings treated with each isomer to identify isomer-specific changes in protein abundance and to investigate the potential biological roles of different isomers. Additionally, we employed electrophysiological approaches to evaluate the effects of both isomers on net ion transport and cyclic nucleotide-gated channels 2 and 18 (CNGC2 and CNGC18) [13]. Our findings provide novel insights into common and distinct molecular and physiological roles of the two cAMP isomers in plant signalling.

Material and Methods

Plant material

A. thaliana (Columbia ecotype) seeds were surface-sterilized using 70% ethanol (v/v) and 60% bleach (v/v) and then washed five times in sterile water. After two days of stratification in darkness at 4 °C, seeds were inoculated into liquid Murashige and Skoog (MS) medium supplemented with 1% (w/v) sucrose and maintained under continuous light conditions. The medium was replaced after 7 days, and three days later, when seedlings were 10 days old, they were treated with 0.2 µM of the cell permeant Br-2',3'-cAMP or 0.2 µM Br-3',5'-cAMP [12]Seedlings treated with water served as control. After 3 hours of treatment, the seedlings were harvested, washed with distilled water for 5 minutes, dried on paper, and flash-frozen in liquid nitrogen; they were then stored at -80°C.

Workflow of the proteomics analysis

The frozen plant material was ground to a fine powder with liquid nitrogen, and proteins were extracted using the SDS/phenol method [14] and digested with trypsin via Filter Aided Sample Preparation (FASP) [15]. Peptides were analysed by LC-MS/MS as detailed elsewhere [16]. MS/MS spectra were searched against the *A. thaliana* proteome database (TAIR10, containing 48,266 entries; http://www.arabidopsis.org) using MaxQuant software (version 1.6.10.43) with default parameters (https://www.maxquant.org). For the quantitative proteome, the 'ProteinGroups' output file generated by the MaxQuant search was loaded into Perseus software (version 1.6.15.0).

Control versus (vs) 2'3'-cAMP and control vs 3'5'-cAMP treated samples were compared. The two original complete data sets, containing log2-transformed intensities, were split into three subsets each, based on the percentage of replicates with missing or valid values per treatment with a threshold of 75% as described in Supplementary Protocol (Supplementary file 1 and Fig. S1).

Analyses and data visualization

To generate networks for known and predicted protein–protein interactions, the data sets were loaded to the STRING database (https://string-db.org; version 10.5) using a high confidence interaction score (>0.7). As active interaction sources, text mining, experiments, databases, co-expression, neighbourhood, gene fusion, and co-occurrence were selected. Proteins that did not interact with any other proteins were removed from the network. The network was imported in Cytoscape (version 3.10.3) for protein visualization: we created a clustered version of the network with MCL, and for each cluster, we retrieved enriched functional annotation using the functional enrichment String tool embedded in Cytoscape with default parameters. Only networks with more than three interactions were retained. GO enrichment analysis was conducted using ShinyGO V0.82 (https://bioinformatics.sdstate.edu/go) with the entire species as the background and a p-value cut-off of 0.05. Venn diagrams were created using the Venny 2.1 online tool

(http://bioinfogp.cnb.csic.es/tools/venny). To identify potential regulatory mechanisms, transcription factor binding sites (TFBS) within the 1000 bp upstream regions of genes encoding DAPs were analyzed using the web server (http://acrab.cnb.csic.es/TDTHub/; accessed July 1, 2025) TFBS-Discovery Tool Hub (TDTHub) [17]. The analysis used *A. thaliana* as the reference species and the FIMO algorithm for TFBS mapping, with a minimum S-Score threshold set at 5%.

Non-invasive Microelectrode Ion Flux Estimation (MIFE) measurement

The net ion fluxes were measured using the non-invasive MIFE technique (University of Tasmania, Hobart, Australia). Specific details on electrode fabrication, calibration, and sample preparation are given elsewhere [18]. Roots of ten-day-old seedlings were immobilized on a cover slide with parafilm strips and immersed in a Petri dish filled with basic salt medium (BSM) solution (0.5 mM KCl and 0.1 mM CaCl2, pH 5.7). K^+ and Ca^{2+} net fluxes were measured from the root mature zone for 5 minutes as the initial steady state before the application of cAMP. Then, the K^+ and Ca^{2+} fluxes in response to 10 µM of 8-Br-3',5'-cAMP or 8-Br-2',3'-cAMP were monitored for an additional 10 minutes. To investigate the effect of exogenous cAMP on oxidative stress responses, K^+ and Ca^{2+} net fluxes in response to transient 10 mM H_2O_2 were measured from roots of seedlings that were pretreated with or without 8-Br-3',5'-cAMP or 8-Br-2',3'-cAMP.

Preparation of CNGC2 and CNGC18 encoding mRNA

CNGC2 (At5g15410) and CNGC18 (At5g14870) cDNA were synthesised by VectorBuilder and inserted into the pT7 vector within the flanking region of the globin gene of *X. laevis*. The cDNA was amplified in *E. coli* and purified with the Wizard® Plus SV Minipreps DNA Purification System. CNGC2 and CNGC18 cDNAs were linearized by AscI or SgsI, respectively. Corresponding cRNAs were capped and transcribed *in vitro* and using T7 RNA polymerase [19].

Heterologous protein expression and two-electrode voltage clamp (TEVC) electrophysiology

Electrophysiological recordings were performed in *X. laevis* oocytes purchased from Ecoocyte Bioscience GmbH (Dortmund, Germany). Healthy and full-grown oocytes were microinjected with 25ng/50nL purified cRNA encoding CNGC2 and CNGC18 with a manual microinjection system (Drummond Scientific Company, Broomall, PA, USA). Oocytes were subsequently incubated at 18°C for 3-5 days in NDE solution (96 mM NaCl, 2 mM KCl, 1 mM $MgCl_2$, 5 mM 4-(2-hydroxyethyl)-1-piperazineethanesulfonic acid (HEPES) 2.5 mM pyruvate, 0.05 mg/mL gentamicin sulphate, and 1.8 mM $CaCl_2$ at pH 7.6) to allow for heterologous expression of CNGC2 and CNGC18. The electrophysiological measurements were performed using a two-electrode voltage clamp (TEVC) at controlled voltage conditions with the Oocyte Clamp OC-725C or B amplifier (Warner Instruments, Hamden, CT, USA). The digitally recorded currents were collected using the pCLAMP software (Version 11.2.2, Molecular Devices, San Jose, CA, USA). The two microelectrodes were filled with 3 M KCl, and bath electrodes were connected to the oocyte chamber via two agar bridges (3% agar in 3 M KCl). To measure K^+-currents, the external control solution contained 96 mM KCl, 1.8 mM $CaCl_2$, 1.8 mM $MgCl_2$, and 10 mM HEPES-KOH, pH 7.5. The Ca^{2+}-currents were measured using an external control solution composed of 10 mM $CaCl_2$, 185 mM D-mannitol, and 10 mM MES-Tris, pH 7.4. The current-voltage (I-V) relationship was obtained using a voltage jump protocol consisting of 10 square pulses (0.8 s long) ranging from -180 mV to 0 mV (in 20 mV increments) before and after incubation (30 minutes) with 50µM of either 8-Br-3',5'-cAMP or 8-Br-2',3'-cAMP

Statistical analysis

For proteomic analysis the statistical workflow was performed as described previously [20]: In brief, only the subset 1, obtained as described in Supplementary Protocol (Supplementary file 1), was centred around zero by subtracting the median within each replicate (n = 4) and subjected to a two-sample t-test ($P < 0.05$).

For MIFE technique, the statistical significance in H_2O_2-induced ion fluxes was determined by One-way ANOVA, Šídák's multiple comparisons ($p < 0.05$).

For electrophysiology analysis the data were collected using Clampfit 11.2.2 software (Molecular Devices, Sunnyvale, CA, USA). OriginPro 8.0 (OriginLab Corp., Northampton, MA, USA). OriginPro 8 and GraphPad Prism 8.0.2 (GraphPad Software, Boston, MA, USA) were used for statistical analyses. The statistical significance of the data was determined using the unpaired *t*-test. Levels of significance were defined as *, $p < 0.05$; **, $p < 0.01$; ***, $p < 0.001$; ****, $p < 0.0001$. The number of oocytes (n) obtained from a frog (N) used in each experiment is indicated as "n/N".

Results

Early changes in the proteome in response to cAMP isomers

To gain insight into early systemic changes elicited by the two cAMP isomers, we focused on changes in the proteome of *A. thaliana* seedlings after three hours of exposure to cell-permeant derivatives of 3',5'-cAMP or 2',3'-cAMP. Proteomic analysis of control and cAMP-treated samples identified 5614 protein groups in total (Tab. S1). We applied a hybrid analytical approach that separately considers intensity-based and presence/absence data [20] and categorized the dataset into three subsets (Fig. S1, Supplementary file 1). In subset 1, we included proteins with sufficient quantitative data for statistical analysis. Subset 2 contained proteins with unreliable or inconsistent detection levels, and subset 3 contained "unique" proteins that were present under one condition only (either treatment or control). Furthermore, we classified the differentially abundant proteins (DAPs, Tab. S2 and S3) in up-regulated (detected only or significantly more abundant in cAMP-treated samples) and down-regulated proteins (detected only in control samples or significantly more abundant under control conditions). In a total of 168 DAPs in 3',5'-cAMP-treated plantlets, 97 were upregulated and 71 were downregulated. In 168 DAPs identified from the 2',3'-cAMP-treated plantlets, 49 were upregulated and 119 were downregulated. A Venn diagram revealed that only 33 DAPs are shared between the two treatments (Fig. 4A, Tab. S4). The majority of common proteins are annotated as having roles in metabolic processes, including protein metabolism and response to stimuli (Fig. 4B, Tab. S4).

Gene Ontology (GO) enrichment analysis of the DAPs was conducted using ShinyGO V0.82 (based on Ensembl Release 104, Feb. 3, 2025) [21] (Fig. 4C). Biological process analysis showed that DAPs linked to 3',5'-cAMP treatment were enriched in cellular component organization or biogenesis. In terms of cellular component enrichment, these DAPs were associated with the Golgi apparatus, cytosol, mitochondrion, and plastid. No significant enrichment was observed for molecular functions. In turn, DAPs from the 2',3'-cAMP treatment were significantly enriched in biological processes such as purine nucleobase catabolic process, quinone metabolic process, vesicle-mediated transport, and translation. (Fig. 4C). Cellular components analysis revealed enrichment in the ribosome, vesicle membrane, cytosol, and mitochondrion. Molecular function enrichment indicated that these DAPs were involved in ureide hydrolase activity, structural components of the ribosome, and mRNA binding.

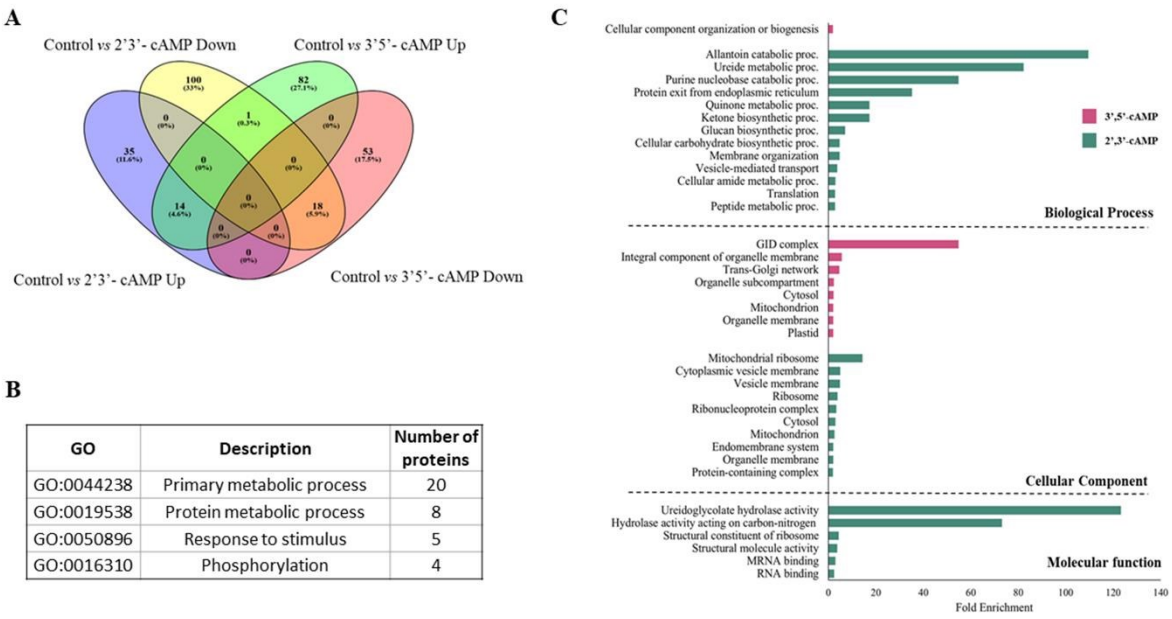

B

GO	Description	Number of proteins
GO:0044238	Primary metabolic process	20
GO:0019538	Protein metabolic process	8
GO:0050896	Response to stimulus	5
GO:0016310	Phosphorylation	4

Fig.4 A comparative proteomics after 2′,3′-cAMP and 3′,5′-cAMP treatment. **A.** Venn diagram showing the overlap of significantly regulated proteins following 0,2 µM Br-2′,3′-cAMP or Br-3′,5′-cAMP treatment. **B.** Functional classification of the shared DAPs. **C.** Gene Ontology term enrichments of biological process, cellular Additional, and molecular function were significantly overrepresented among the differentially abundant proteins (FDR-corrected $p \leq 0.05$, n = 4 biological replicates).

To gain further insight into the relationships among the DAPs in response to the isomers, we constructed a protein-protein interaction (PPI) network using String with a high confidence interaction score. This analysis revealed that the majority of interacting DAPs in both treatments were associated with translation, RNA binding, and ribosomal activity (Fig. 5). Notably, 3′,5′-cAMP treatment led to an increased abundance of the proteins related to these processes, whereas 2′,3′-cAMP treatment decreased the abundance of proteins involved in these functions. Additional cluster associated with ribosome biogenesis was specifically linked to 3',5'-cAMP (Fig. 5A), whereas the 2,3'-cAMP-associated DAPs formed clusters related to splicing and ribonucleoprotein complexes, oxidative phosphorylation, and vesicle-mediated transport (Fig. 5B).

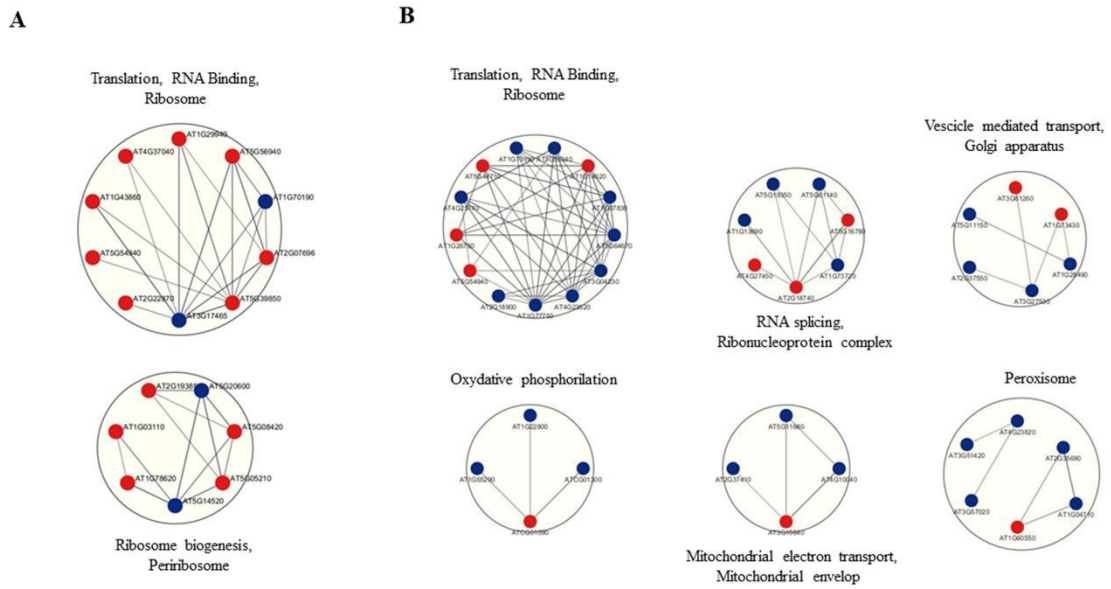

Fig. 5 Functional protein-protein interaction networks. **A**. DAPs induced by 3'5'-cAMP **B**. DAPs induced by 2'3'- cAMP. DAPs upregulated were indicated with red circles, while the downregulated were shown with blue circles.

To infer common and specific cAMP-isomer-dependent mechanisms, transcription factor-binding sites in the upstream regions of genes encoding differentially accumulated proteins were analyzed using the TFBS-Discovery Tool Hub (TDTHub) web server [17]. Upstream regions of genes encoding unique 3',5'-cAMP-upregulated DAPs appear significantly enriched in consensus *cis*-elements for transcription factors, including CMTA3, DOF5.4, and GBF1. In contrast, no significant enrichment was observed in the upstream regions of genes encoding the 2',3'-cAMP-upregulated DAPs (Tab. S5).

3',5'- and 2',3'-cAMP modulate oxidative stress-induced K^+ and Ca^{2+} net fluxes in *A. thaliana* roots

To explore the physiological roles of the two cAMP isomers on Arabidopsis roots, the MIFE technology for non-invasive ion flux measurements was applied to monitor real-time net fluxes of K^+ and Ca^{2+} from the mature root zone with high temporal resolution (5 seconds). Seedlings were preincubated for 30 minutes with either isomer or with a control (BMS) solution under non-stress conditions. No difference in basal levels of K^+ or Ca^{2+} fluxes between controls and roots treated with either 3',5'-cAMP or 2',3'-cAMP was found (Fig. 6 inset). Roots' exposure to oxidative stress resulted in a massive net K^+ loss and Ca^{2+} uptake (Fig. 6). Root pretreatment with either 3',5'-cAMP or 2',3'-cAMP significantly attenuated H_2O_2-induced ion fluxes, reducing the response magnitude to approximately 50% of that observed in untreated (mock control) roots (Fig. 6). These findings demonstrate that both isomers can directly or indirectly modulate net fluxes and mitigate ionic imbalances caused by H_2O_2.

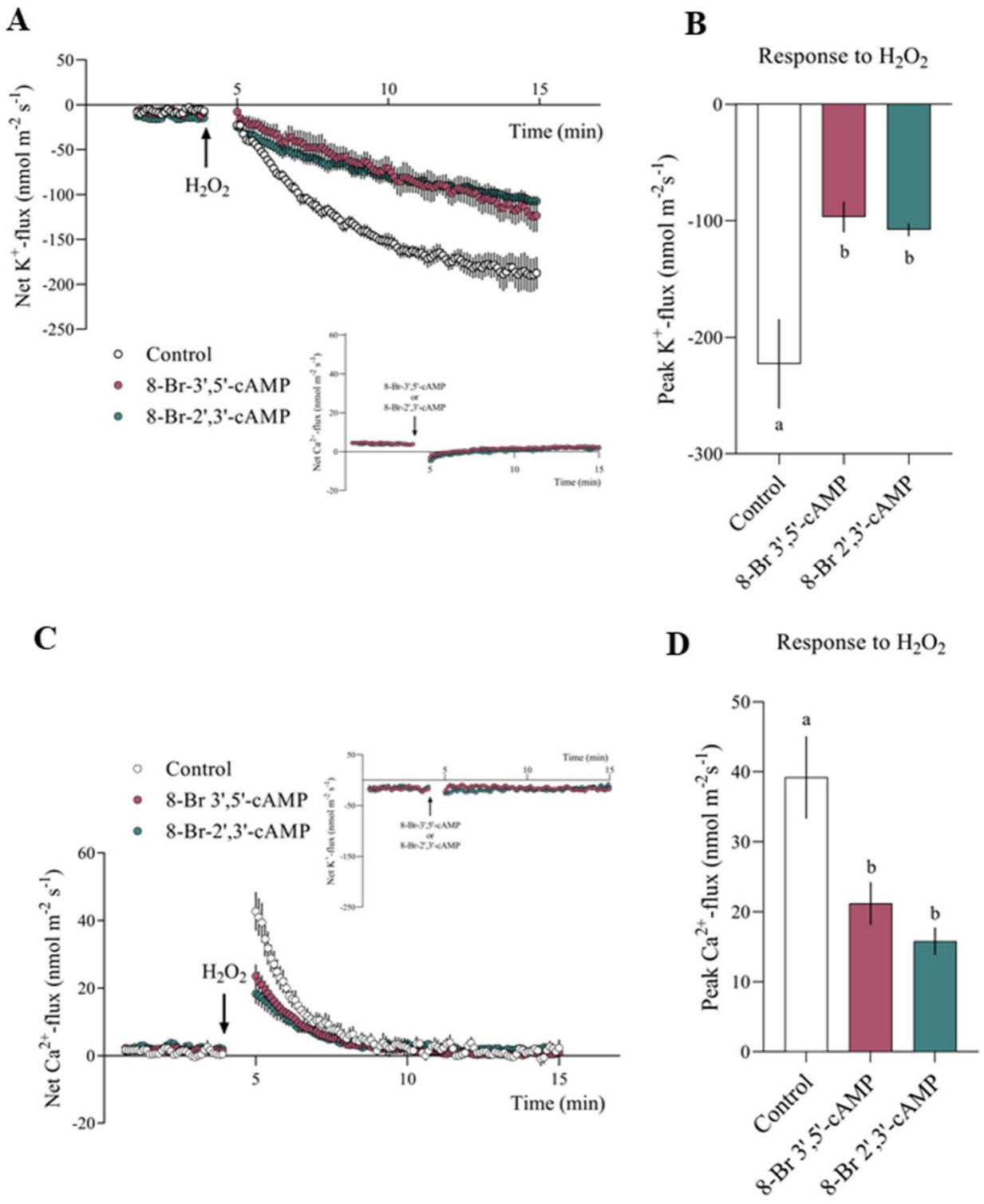

Fig.6 Modulatory effects of 2',3'- and 3',5'-cAMP on H_2O_2-induced ion fluxes in *A. thaliana* roots. **A**: Transient K^+ flux; **B**: peak of net K^+ efflux (nmol m^{-2} s^{-1}); **C**: Transient Ca^{2+} flux; **D:** peak of net Ca^{2+} flux (nmol m^{-2} s^{-1}). Data are mean ± S.E. (n= 5-9 individual plants). Transient treatment with solely 8-Br-3',5'-cAMP or 8-Br-2',3'-cAMP didn't affect ion fluxes (insets of net K^+ and Ca^{2+} flux graphs). Different lowercase letters indicate a significant difference in H_2O_2-induced ion fluxes at $p < 0.05$ (One-way ANOVA, Šídák's multiple comparisons test). The sign convention of ion flux is "negative efflux".

Testing the cAMP isomers as modulators of CNGC2 and CNGC18

CNGC2 and CNGC18 have been reported to be gated by 3', 5'-cAMP when expressed in *X. laevis* oocytes [22]. This is likely due to the presence of a conserved region, the phosphate binding cassette (PBC), which interacts with the sugar and phosphate moieties of cNMP ligands. A "hinge" region between the PBC and the CaMBD may contribute to ligand binding efficacy and selectivity [13]. Since the PBC binds exclusively to the sugar and the phosphate group of cNMPs, it may represent a specific target for only one isomer. Here, we employed an electrophysiological approach to determine if the response to cAMP in these two CNGCs is isomer-specific.

To test this, RNA encoding for CNGC2 or CNGC18 channel was injected into Xenopus oocytes, and whole-cell current recorded by TEVC using a voltage step protocol from the holding potential of -60 mV (20 mV step, from –180 mV to 0 mV) (Fig. 7). Since acute perfusion with 3′,5′-cAMP in the recording chamber, was insufficient to elicit any currents, we employed a pre-incubation protocol [22] in which oocytes expressing the channel were incubated for 30 minutes with either 50 μM of 3′,5′-cAMP or 50 μM 2′,3′-cAMP. Currents of CNGC2 and CNGC18 expressing oocytes were recorded before and after the incubation. In the oocytes expressing both CNGC2 and CNGC18, an inward cationic current was observed following incubation with 3′,5′-cAMP, both in the presence of either K^+ (96 mM KCl; Fig. 7A-7C-red) or Ca^{2+} (10 mM CaCl; Fig. 7B-7D red).

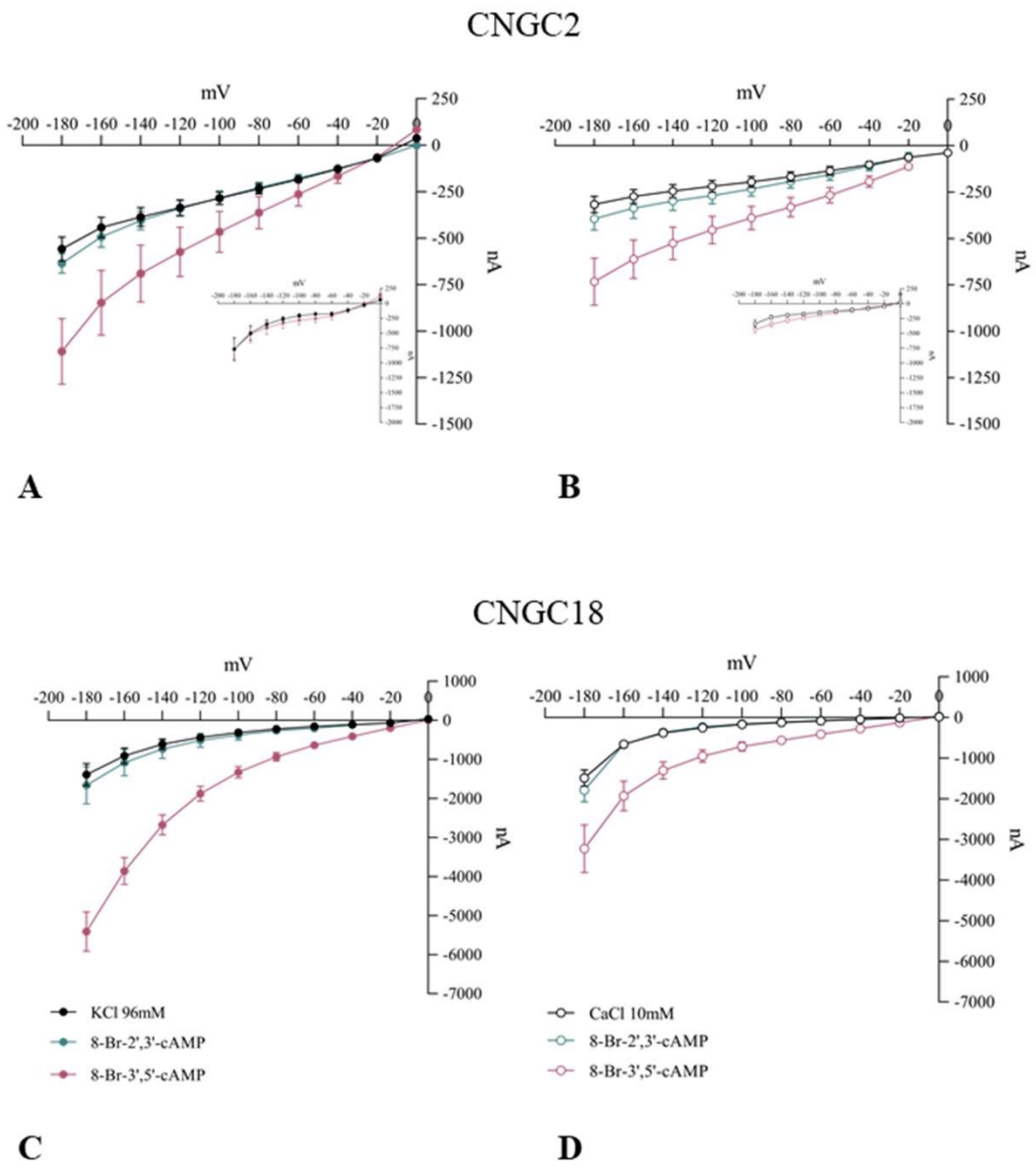

Fig.7 CNGC2 and CNGC18 are activated by 3′5′-cAMP but not by 2′3′-cAMP. **A-B** I-V relationship recorded in oocytes expressing CNGC2 under the same conditions as in A. (n/N=15/2; n/N=11/2) and B. (n/N=13/2; n/N=11/2). Non-injected oocytes exhibit no response to 3′5′-cAMP under either condition (insets of K^+- and Ca^{2+}-current graphs). **C** I-V relationship (from -140 mV to 0 mV) in oocytes expressing CNGC18 shows inward K^+-currents in response to 3′5′-cAMP (n/N=11/2), while no activation is observed with 2′3′-cAMP (filled dots) (n/N=9/2). **D** As in A., Ca^{2+} -currents (open dots) are observed with 3′5′-cAMP (n/N = 8/2) but not with 2′3′-cAMP (n/N = 10/2).

When the ligand was 2′,3′-cAMP, however, no current was observed (Fig. 8). This is clearly visualized by analyzing the net current values obtained by subtracting the baseline current recorded from the current recorded after 30 minutes (Fig. 8). As expected, non-injected oocytes did not show any response after the incubation in 3′,5′-cAMP either in Ca^{2+}- or K^+-containing solutions (Fig. 8 inset). In order to further define the current activation lag phase, we performed a time course by microinjecting 50 nL of 3',5'-cAMP (50 µM) into oocytes expressing CNGC2 and monitoring the K^+ current (96 mM KCl) at 10-minute intervals. Under these conditions, we observed maximal channel opening between 20 and 40 minutes (data not shown). Doubling the amount of 3',5'-cAMP (100 µM) did not shorten the lag phase.

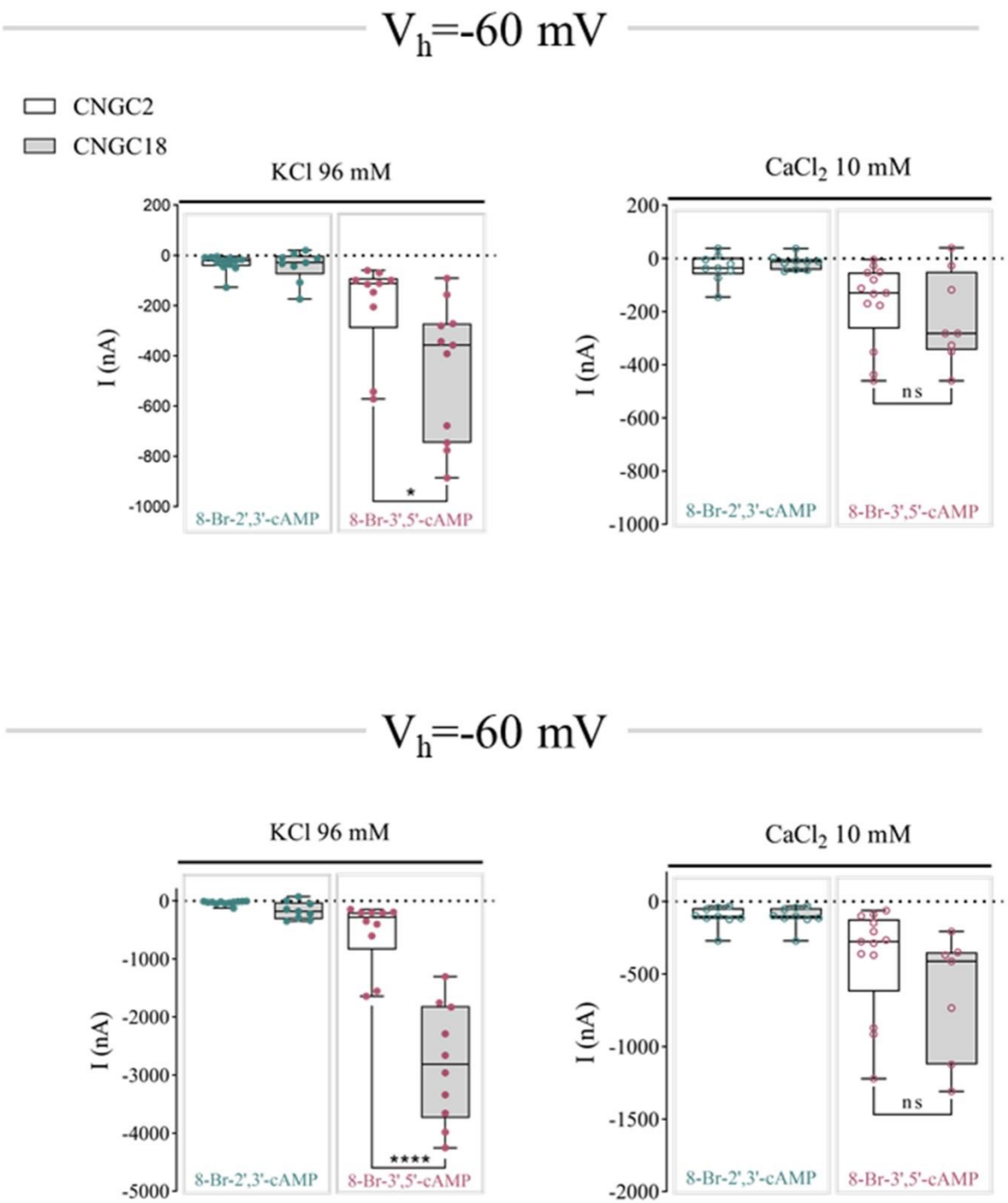

Fig. 8 Box-plots representing the current amplitudes elicited in oocytes after 30 min of incubation in 2'3'cAMP and 3'5'cAMP. The net currents were calculated by subtracting the basal current (recorded in the presence of KCl 96mM or $CaCl_2$ 10mM) from the substrate-induced current.

Discussion

The cyclic nucleotide isomers 3′,5′-cAMP and 2′,3′-cAMP differ markedly in their biosynthetic origins. The 3′,5′-cAMP isomer is produced by ACs, which in plants are often embedded within multifunctional proteins [23–27]. Some of these ACs can be activated as part of receptor-linked responses to diverse extracellular cues, positioning 3′,5′-cAMP as a localized and dynamic signal that regulates key physiological processes, including ion homeostasis, stomatal movement, pollen tube growth, and stress adaptation [28, 29]. In contrast, 2′,3′-cAMP is generated during RNA degradation and is therefore enhanced under stress conditions, such as wounding, heat, or hypoxia, resulting in increased intracellular levels of 2′,3′-cAMP [9, 30, 31]. The link between stress-induced RNA turnover and 2′,3′-cAMP accumulation may indicate a role as a cellular effector or response metabolite, rather than as a signalling molecule in the classical sense. 2′,3′-cAMP may provide and quantitative, dose response-like link to stress damage, also raising the possibility that 2',3'-cAMP functions in cellular protection and metabolic adaptation. The discovery that Toll/Interleukin-1 receptor (TIR) domains can act as 2′,3′-cAMP/cGMP synthetases by hydrolysing RNA/DNA implies that this isomer may be generated in highly regulated signalling contexts, particularly in plant immunity [32]. Furthermore, in plants the presence of both isoform-specific and dual-specificity phosphodiesterases [33–36] is consistent with the calibration of isomer levels and, consequently, the tuning of their downstream effects.

Our systems-level analysis, conducted using proteomics, has revealed that the two cAMP isomers result in a markedly different set of DAPs, with just 20% of proteins shared. This implies that both isomers largely affect specific biological pathways and GO enrichment and PPI analyses emphasize this difference. Notably, the 3′,5′-isomer predominantly influenced target proteins associated with roles in cellular component organization and biogenesis, process typically linked to the regulation of growth and development. The 2',3’-isomer affects proteins with a role in purine nucleobase catabolism, which could be interpreted as a feed-back stimulation in response to the nucleotide addition and suggests that stress-induced RNA degradation producing 2',3'-cAMP will eventually also stimulate nuclease degradation to prevent flooding the system with 2',3'-cAMP. The isomer effect of quinone metabolism is also noteworthy given their role in cellular respiration, photosynthesis, the metabolism of xenobiotics, and the production of phenylpropanoids. Importantly, quinones serve as key redox-active compounds. Their dual nature enables them to generate reactive oxygen species (ROS), which can cause oxidative damage, but they also function as antioxidants and signalling molecules, helping plants detect and respond to stress [37, 38].

Changes in the vesicle-mediated transport are also part of systemic stress responses that, in turn, cause elevated cellular 2',3'-cAMP levels [39, 40]. The regulation of transcription is also a systems-level response, and again significantly affected by 2',3'-cAMP treatment. The prominence of RNA-binding proteins in the 2′,3′-cAMP-treated samples is entirely consistent with previous reports linking this isomer to stress granule dynamics and mRNA turnover [10, 12]. PPI analysis supports these connections and points to the operation of networks that integrate translation, RNA binding, and ribosomal function. Additional clusters unique to 2′,3′-cAMP included splicing and ribonucleoprotein complex formation, which is again diagnostic for a systemic effect of 2′,3′-cAMP on RNA processing. Finally, the downregulation of proteins involved in oxidative phosphorylation and mitochondrial transport has also been observed in animal cells, where elevated levels of 2′,3′-cAMP have been implicated in mitochondrial dysfunction [41]. Furthermore, transcription factor (TF) binding site analyses again point to distinct mechanisms of action for the two isomers. Upstream regions of genes encoding 3',5'-cAMP-upregulated DAPs appear significantly enriched in *cis*-elements for transcription factors, including CMTA3, DOF5.4, and GBF1. These *cis*-elements are not enriched in genes encoding 2',3'-cAMP-upregulated DAPs. Notably, the calmodulin-binding transcription factor CMTA3 had previously been proposed as a TF regulated by 3',5'-cAMP during the Arabidopsis immune response [42].

To further study the system-wide effects of two cAMP isomers, we quantified the ion net fluxes from roots. Extensive literature exists regarding the impact of 3',5'-cAMP on ionic flux under stress conditions [43]. However, no such data are available for 2',3'-cAMP. It is well established that ROS can activate both outward-rectifying potassium channels and non-selective cation channels (NSCCs) in the root epidermis, and this can cause net K^+ efflux and Ca^{2+} influx [44–46]. ROS-mediated channel activation is essential in early stress responses and can contribute to physiological adaptation. In our study, a pre-treatment with either 2′,3′- or 3′,5′-cAMP significantly reduced H_2O_2-induced K^+ efflux and Ca^{2+} influx, and this is

consistent with cAMP-dependent ROS-activated ion transport. Both isomers cause similar changes to the net-flux signature and may do so via common and/or at least partly different pathways.

In order to assess specific and direct effects of the isomers, we turned to the CNGCs. A hallmark of the 3',5'-cAMP signaling in plants is its capacity to enable ion flux through specific CNGCs [13], such as CNGC2 and CNGC18 [47, 48], which have a role in various physiological responses, including immune signaling and pollen tube guidance. To date, reports of cAMP effects on CNGCs have considered the 3′,5′-cAMP isomer only. Here, we have been able to elicit inward cationic currents in Xenopus oocytes expressing either CNGC2 or CNGC18 from *A. thaliana* in the presence of the 3′,5′-cAMP. In contrast, 2′,3′-cAMP failed to induce any measurable current, and this provides direct functional evidence for isomer-specific cAMP responses and suggests that AC activation is an essential upstream part of cAMP-dependent CNGC modulation.

Interestingly, we observed a reproducible lag phase, also when the cAMP was injected, before the activation of 3′,5′-cAMP-induced currents. This phenomenon has already been observed in guard cell protoplasts under similar experimental conditions in the whole-cell configuration[49]. The authors have speculated that the long incubation times required for ligand activation could be due to competition for binding sites between cAMP and CaM. In plant CNGCs, these sites are both located in the C-terminal domain, differing from the animal CNGC configurations. The authors propose that a further reason might be that plant cells have comparatively relatively higher levels of cyclic nucleotide phosphodiesterases than animal cells; however, this point is not relevant in our oocyte system, in which we use non-hydrolyzable cAMP as well as a heterologous animal system. It appears more likely that the lag may be caused by the time required for cAMP to diffuse in a crowded cytoplasmic microenvironment and to reach and saturate the binding sites. Furthermore, these findings are also consistent with the idea that cyclic nucleotide signalling in plants operates within spatially restricted cellular microenvironments where cAMP signalling is tightly localized to prevent non-specific activation and to ensure signal fidelity [29]. In the context of plant cells, membrane nanodomains and localized pools of cyclic nucleotide-producing enzymes likely contribute to this compartmentalization, where, e.g., moonlighting ACs are located close to cAMP-dependent proteins like CNGCs. The Xenopus oocyte system lacks such spatial constraints, which may account for the observed kinetic delay and provide further support for the physiological relevance of localized signalling *in vivo*.

In summary, our data show that both isomers directly or indirectly cause distinct systemic effects on the proteome, with the 2',3' isomer affecting systems-level functions such as transcriptional regulation. None of the isomers affects net ion fluxes in the root under control conditions, but both elicit the same response under H_2O_2 stress conditions. The mechanisms by which this occurs will need to be elucidated. Finally, the cAMP gating effect on CNGC2 and CNGC18 is 3',5'-AMP isomer-specific and, hence, dependent *in vivo* on activated adenylate cyclases.

Supplementary file 1. Supplementary Protocol.

Supplementary Figure S1. Filtering data system.

Supplementary Table S1-S4. Total dataset, DAPs and shared DAPs.

Supplementary Table S5. Transcription factor-binding sites enrichment analysis.

Acknowledgements

E.D. is a Ph.D. student of the “Life Sciences and Biotechnology” course at University of Insubria.

This work was supported by the University of Insubria grant “Fondo di Ateneo per la Ricerca 2024 and 2025” (to B.M. and C.V.).

Proteomics was performed with the support of the Functional Genomics Center Zurich (FGCZ) of University of Zurich and ETH Zurich.

Authors' contributions

ED and ADI: In Vivo Experiments, Data Collection, Original Draft

ED, ADI and PY: Data analysis;

ED, ADI and SS: Validation;

MM and GD: Software, Computational Analysis, Visualization;

EB and SS: Resources;

CV, CG and EB: Conceptualization;

EB: Methodology Writing;

EB, PY, SS, CV and CG: Writing– Review & Editing;

MB and CV: Funding Acquisition;

PY, SS, CV and CG: Supervision.

Conflict of Interest

No conflict of interest declared.

Funding

This work was supported by the University of Insubria grant Fondo di Ateneo per la Ricerca 2024 and 2025 (to B.M. and C.V.).

Data Availability

The mass spectrometry data have been deposited to the ProteomeXchange Consortium (http://proteomecentral.proteomexchange.org) via the jPOST partner repository (https://repository.jpostdb.org) with the data set identifier PXD066253 for ProteomeXchange and JPST003946 for jPOST

References

1. Kurosaki F, Nishi A. Stimulation of Calcium Influx and Calcium Cascade by Cyclic AMP in Cultured Carrot Cells. Arch Biochem Biophys. 1993;302:144–51. https://doi.org/10.1006/ABBI.1993.1192.

2. Jin XC, Wu WH. Involvement of cyclic AMP in ABA- and Ca2+-mediated signal transduction of stomatal regulation in Vicia faba. Plant Cell Physiol. 1999;40:1127–33. https://doi.org/10.1093/oxfordjournals.pcp.a029497.

3. Li W, Luan S, Schreiber SL, Assmann SM. Cyclic AMP stimulates K+ channel activity in mesophyll cells of Vicia faba L. Plant Physiol. 1994;106:957–61. https://doi.org/10.1104/pp.106.3.957.

4. Tezuka T, Akita I, Yoshino N, Suzuki Y. Regulation of self-incompatibility by acetylcholine and cAMP in Lilium longiflorum. J Plant Physiol. 2007;164:878–85. https://doi.org/10.1016/j.jplph.2006.05.013.

5. Maathuis FJM, Sanders D. Sodium uptake in Arabidopsis roots is regulated by cyclic nucleotides. Plant Physiol. 2001;127:1617–25. https://doi.org/10.1104/pp.010502.

6. Zhao J, Guo Y, Fujita K, Sakai K. Involvement of cAMP signaling in elicitor-induced phytoalexin accumulation in Cupressus lusitanica cell cultures. New Phytologist. 2004;161:723–33. https://doi.org/10.1111/j.1469-8137.2004.00976.x.

7. Pietrowska-Borek M, Nuc K. Both cyclic-AMP and cyclic-GMP can act as regulators of the phenylpropanoid pathway in Arabidopsis thaliana seedlings. Plant Physiology and Biochemistry. 2013;70:142–9. https://doi.org/10.1016/j.plaphy.2013.05.029.

8. Zhao Y, Liu Y, Ji X, Sun J, Lv S, Yang H, et al. Physiological and proteomic analyses reveal cAMP-regulated key factors in maize root tolerance to heat stress. Food Energy Secur. 2021;10:1–24. https://doi.org/10.1002/fes3.309.

9. Van Damme T, Blancquaert D, Couturon P, Van Der Straeten D, Sandra P, Lynen F. Wounding stress causes rapid increase in concentration of the naturally occurring 2′,3′-isomers of cyclic guanosine- and cyclic adenosine monophosphate (cGMP and cAMP) in plant tissues. Phytochemistry. 2014;103:59–66. https://doi.org/10.1016/j.phytochem.2014.03.013.

10. Kosmacz M, Luzarowski M, Kerber O, Leniak E, Gutiérrez-Beltrán E, Moreno JC, et al. Interaction of 2',3'-cAMP with Rbp47b Plays a Role in Stress Granule Formation. Plant Physiol. 2018;177:411–21. https://doi.org/10.1104/pp.18.00285.

11. Luo W, Xu Y, Cao J, Guo X, Han J, Zhang Y, et al. COLD6-OSM1 module senses chilling for cold tolerance via 2′,3′-cAMP signaling in rice. Mol Cell. 2024;84:4224-4238.e9. https://doi.org/10.1016/j.molcel.2024.09.031.

12. Chodasiewicz M, Kerber O, Gorka M, Moreno JC, Maruri-Lopez I, Minen RI, et al. 2′,3′-cAMP treatment mimics the stress molecular response in Arabidopsis thaliana. Plant Physiol. 2022;188:1966–78. https://doi.org/10.1093/plphys/kiac013.

13. Zelman AK, Dawe A, Gehring C, Berkowitz GA. Evolutionary and structural perspectives of plant cyclic nucleotide-gated cation channels. Front Plant Sci. 2012;3 MAY:1–13. https://doi.org/10.3389/fpls.2012.00095.

14. Vannini C, Domingo G, Fiorilli V, Seco DG, Novero M, Marsoni M, et al. Proteomic analysis reveals how pairing of a Mycorrhizal fungus with plant growth-promoting bacteria modulates growth and defense in wheat. Plant Cell Environ. 2021;44:1946–60. https://doi.org/10.1111/pce.14039.

15. Wiśniewski JR. Filter Aided Sample Preparation – A tutorial. Anal Chim Acta. 2019;1090:23–30. https://doi.org/10.1016/j.aca.2019.08.032.

16. Paradiso A, Domingo G, Blanco E, Buscaglia A, Fortunato S, Marsoni M, et al. Cyclic AMP mediates heat stress response by the control of redox homeostasis and ubiquitin-proteasome system. Plant Cell Environ. 2020;43:2727–42. https://doi.org/10.1111/pce.13878.

17. Grau J, Franco-Zorrilla JM. TDTHub, a web server tool for the analysis of transcription factor binding sites in plants. Plant Journal. 2022;111:1203–15. https://doi.org/10.1111/tpj.15873.

18. Ordoñez NM, Shabala L, Gehring C, Shabala S. Noninvasive microelectrode ion flux estimation technique (MIFE) for the study of the regulation of root membrane transport by cyclic nucleotides. Methods in Molecular Biology. 2013;1016:95–106. https://doi.org/10.1007/978-1-62703-441-8_7.

19. Bhatt M, Di Iacovo A, Romanazzi T, Roseti C, Cinquetti R, Bossi E. The “www” of Xenopus laevis Oocytes: The Why, When, What of Xenopus laevis Oocytes in Membrane Transporters Research. Membranes (Basel). 2022;12. https://doi.org/10.3390/membranes12100927.

20. Nikonorova N, Van Den Broeck L, Zhu S, Van De Cotte B, Dubois M, Gevaert K, et al. Early mannitol-triggered changes in the Arabidopsis leaf (phospho)proteome reveal growth regulators. J Exp Bot. 2018;69:4591–607. https://doi.org/10.1093/jxb/ery261.

21. Ge SX, Jung D, Jung D, Yao R. ShinyGO: A graphical gene-set enrichment tool for animals and plants. Bioinformatics. 2020;36:2628–9. https://doi.org/10.1093/bioinformatics/btz931.

22. Leng Q, Mercier RW, Yao W, Berkowitz GA. Cloning and first functional characterization of a plant cyclic nucleotide-gated cation channel. Plant Physiol. 1999;121:753–61. https://doi.org/10.1104/pp.121.3.753.

23. Al-Younis I, Wong A, Gehring C. The Arabidopsis thaliana K+-uptake permease 7 (AtKUP7) contains a functional cytosolic adenylate cyclase catalytic centre. FEBS Lett. 2015;589:3848–52. https://doi.org/10.1016/j.febslet.2015.11.038.

24. Chatukuta P, Dikobe TB, Kawadza DT, Sehlabane KS, Takundwa MM, Wong A, et al. An arabidopsis clathrin assembly protein with a predicted role in plant defense can function as an adenylate cyclase. Biomolecules. 2018;8:1–15. https://doi.org/10.3390/biom8020015.

25. Al-Younis I, Wong A, Lemtiri-Chlieh F, Schmöckel S, Tester M, Gehring C, et al. The arabidopsis thaliana K+ -uptake permease 5 (AtKUP5) contains a functional cytosolic adenylate cyclase essential for K+ transport. Front Plant Sci. 2018;871 November:1–15. https://doi.org/10.3389/fpls.2018.01645.

26. Bianchet C, Wong A, Quaglia M, Alqurashi M, Gehring C, Ntoukakis V, et al. An Arabidopsis thaliana leucine-rich repeat protein harbors an adenylyl cyclase catalytic center and affects responses to pathogens. J Plant Physiol. 2019;232:12–22. https://doi.org/10.1016/J.JPLPH.2018.10.025.

27. Ruzvidzo O, Gehring C, Wong A. New Perspectives on Plant Adenylyl Cyclases. Front Mol Biosci. 2019;6 December:1–8. https://doi.org/10.3389/fmolb.2019.00136.

28. Blanco E, Fortunato S, Viggiano L, de Pinto MC. Cyclic amp: A polyhedral signalling molecule in plants. Int J Mol Sci. 2020;21:1–2. https://doi.org/10.3390/ijms21144862.

29. Gehring C, Turek IS. Cyclic nucleotide monophosphates and their cyclases in plant signaling. Front Plant Sci. 2017;8 October:1–15. https://doi.org/10.3389/fpls.2017.01704.

30. Thompson JE, Venegas FD, Raines RT. Energetics of Catalysis by Ribonucleases: Fate of the 2′,3′-Cyclic Phosphodiester Intermediate. Biochemistry. 1994;33:7408–14. https://doi.org/10.1021/bi00189a047.

31. Jackson EK, Ren J, Mi Z. Extracellular 2′,3′-cAMP is a source of adenosine. Journal of Biological Chemistry. 2009;284:33097–106. https://doi.org/10.1074/jbc.M109.053876.

32. Yu D, Song W, Tan EYJ, Liu L, Cao Y, Jirschitzka J, et al. TIR domains of plant immune receptors are 2′,3′-cAMP/cGMP synthetases mediating cell death. Cell. 2022;185:2370-2386.e18. https://doi.org/10.1016/j.cell.2022.04.032.

33. Tyc K, Kellenberger C, Filipowicz W. Purification and characterization of wheat germ 2’,3’-cyclic nucleotide 3’-phosphodiesterase. Journal of Biological Chemistry. 1987;262:12994–3000. https://doi.org/10.1016/S0021-9258(18)45156-3.

34. Brown EG, Al-Najafi T, Newton RP. Cyclic nucleotide phosphodiesterase activity in Phaseolus vulgaris. Phytochemistry. 1977;16:1333–7. https://doi.org/10.1016/S0031-9422(00)88777-4.

35. Diffley PE, Geisbrecht A, Newton RP, Oliver M, Smith CJ, Vaughan J, et al. Variation in isomeric products of a phosphodiesterase from the chloroplasts of Phaseolus vulgaris in response to cations. Plant Biosystems - An International Journal Dealing with all Aspects of Plant Biology. 2001;135:143–56. https://doi.org/10.1080/11263500112331350760.

36. Lin PPC, Varner JE. Cyclic nucleotide phosphodiesterase in pea seedlings. Biochimica et Biophysica Acta (BBA) - Enzymology. 1972;276:454–74. https://doi.org/10.1016/0005-2744(72)91007-8.

37. Kozuleva MA, Petrova AA, Mamedov MD, Semenov AY, Ivanov BN. O2 reduction by photosystem I involves phylloquinone under steady-state illumination. FEBS Lett. 2014;588:4364–8. https://doi.org/10.1016/J.FEBSLET.2014.10.003.

38. Lüthje S, Möller B, Perrineau FC, Wöltje K. Plasma membrane electron pathways and oxidative stress. Antioxid Redox Signal. 2013;18:2163–83. https://doi.org/10.1089/ars.2012.5130.

39. Wang X, Xu M, Gao C, Zeng Y, Cui Y, Shen W, et al. The roles of endomembrane trafficking in plant abiotic stress responses. J Integr Plant Biol. 2020;62:55–69. https://doi.org/10.1111/jipb.12895.

40. Sampaio M, Neves J, Cardoso T, Pissarra J, Pereira S, Pereira C. Coping with Abiotic Stress in Plants—An Endomembrane Trafficking Perspective. Plants. 2022;11. https://doi.org/10.3390/plants11030338.

41. Azarashvili T, Krestinina O, Galvita A, Grachev D, Baburina Y, Stricker R, et al. Ca2+-dependent permeability transition regulation in rat brain mitochondria by 2′,3′-cyclic nucleotides and 2′,3′- cyclic nucleotide 3′-phosphodiesterase. Am J Physiol Cell Physiol. 2009;296:1428–39. https://doi.org/10.1152/ajpcell.00006.2009.

42. Sabetta W, Vandelle E, Locato V, Costa A, Cimini S, Bittencourt Moura A, et al. Genetic buffering of cyclic AMP in Arabidopsis thaliana compromises the plant immune response triggered by an avirulent strain of Pseudomonas syringae pv. tomato. Plant Journal. 2019;98:590–606. https://doi.org/10.1111/tpj.14275.

43. Ordoñez NM, Marondedze C, Thomas L, Pasqualini S, Shabala L, Shabala S, et al. Cyclic mononucleotides modulate potassium and calcium flux responses to H2O2 in Arabidopsis roots. FEBS Lett. 2014;588:1008–15. https://doi.org/10.1016/j.febslet.2014.01.062.

44. Demidchik V, Shabala SN, Coutts KB, Tester MA, Davies JM. Free oxygen radicals regulate plasma membrane Ca2+- and K+-permeable channels in plant root cells. J Cell Sci. 2003;116:81–8. https://doi.org/10.1242/jcs.00201.

45. Demidchik V, Cuin TA, Svistunenko D, Smith SJ, Miller AJ, Shabala S, et al. Arabidopsis root K+-efflux conductance activated by hydroxyl radicals: Single-channel properties, genetic basis and involvement in stress-induced cell death. J Cell Sci. 2010;123:1468–79. https://doi.org/10.1242/jcs.064352.

46. Shabala S, Pottosin I. Regulation of potassium transport in plants under hostile conditions: Implications for abiotic and biotic stress tolerance. Physiol Plant. 2014;151:257–79. https://doi.org/10.1111/ppl.12165.

47. Leng Q, Mercier RW, Hua B-G, Fromm H, Berkowitz GA. Electrophysiological Analysis of Cloned Cyclic Nucleotide-Gated Ion Channels. Plant Physiol. 2002;128:400–10. https://doi.org/10.1104/pp.010832.

48. Zhou L, Lan W, Jiang Y, Fang W, Luan S. A calcium-dependent protein Kinase interacts with and activates a calcium channel to regulate pollen tube growth. Mol Plant. 2014;7:369–76. https://doi.org/10.1093/mp/sst125.

49. Ali R, Ma W, Lemtiri-Chlieh F, Tsaltas D, Leng Q, von Bodman S, et al. Death Don’t Have No Mercy and Neither Does Calcium: Arabidopsis CYCLIC NUCLEOTIDE GATED CHANNEL2 and Innate Immunity. Plant Cell. 2007;19:1081–95. https://doi.org/10.1105/tpc.106.045096.

Chapter 4: cAMP-dependent plant heat stress response

Introduction

Heat stress (HS) is a major abiotic factor that negatively affects plant growth, development, and productivity. With the ongoing rise in global temperatures, the frequency and severity of heat waves are increasing, posing significant challenges to agricultural sustainability. HS occurs when ambient temperatures exceed a species-specific threshold for a sufficient duration, disrupting cellular homeostasis and leading to protein denaturation, membrane destabilization, and excessive accumulation of reactive oxygen species (ROS). These effects impair essential physiological processes such as photosynthesis, respiration, and nutrient transport [49].

To counteract these effects, plants activate a highly conserved heat shock response (HSR), which involves the induction of heat shock transcription factors (HSFs) and the synthesis of heat shock proteins (HSPs). HSPs function as molecular chaperones, stabilizing proteins and preventing their aggregation under stress conditions [50]. The initiation of the HSR is mediated by temperature-sensing mechanisms, including changes in membrane fluidity and calcium influx through cyclic nucleotide-gated channels (CNGCs), which trigger HSF activation and downstream protective pathways [51]. Thermosensory components such as phytochrome B also contribute by integrating light and temperature signals to regulate developmental responses like thermomorphogenesis [52].

In addition to the classical HSR, plants utilize intricate signaling networks to fine-tune their adaptive mechanisms. During HS, ROS are generated in multiple cellular compartments, including through the activity of plasma membrane-localized NADPH oxidases [39, 53]. Although ROS can be damaging, they also function as key signaling molecules that regulate gene expression and activate antioxidant defense systems [39]. The dual role of ROS, as both harmful agents and signaling mediators, depends on a delicate balance between their production and scavenging across cellular compartments [40, 54]. Antioxidants, including enzymes such as superoxide dismutase (SOD), catalases (CAT), ascorbate peroxidases (APX), and low molecular weight metabolites, like ascorbate (ASC), glutathione (GSH),tocopherols and carotenoids, are represent first line of defense against oxidative stress and are essential for maintaining redox homeostasis [38]. Consequently, not only ROS accumulation but also heat-induced redox shifts are closely linked to the HSR, which is critical for thermotolerance [39]. The dynamic interplay among heat shock factors (HSFs), heat shock proteins (HSPs), and ROS-scavenging systems is fundamental for plant acclimation and survival under heat stress conditions [39, 54].

Hormonal crosstalk involving abscisic acid (ABA), ethylene, brassinosteroids, and salicylic acid further refines the HSR by interacting with transcriptional regulators to modulate stress-responsive gene networks and promote adaptive growth changes [39, 49].

Emerging evidence highlights the role of 3',5'-cyclic adenosine monophosphate (cAMP) as a key second messenger in plant thermotolerance. This molecule regulates a wide range of cellular processes, including mRNA translation, vesicle trafficking, autophagy, and ion homeostasis [21, 32]. In tobacco BY-2 cells, cAMP contributes to thermotolerance by maintaining redox homeostasis through the modulation of antioxidant enzymes activity and by regulating the ubiquitin-proteasome system, which is essential for protein quality control. These mechanisms help preserve cellular integrity and prevent oxidative damage during HS [37]. In maize, a functional connection between ABA and cAMP signalling has been demonstrated in the context of the HS. ABA activates a specific adenylyl cyclase, resulting in elevated cAMP levels that enhance antioxidant defences and support cellular homeostasis [30]. Furthermore, exogenous application of cAMP has been shown to improve root thermotolerance by modulating the expression of stress-responsive proteins, including HSPs and ROS-scavenging enzymes [30]. These findings suggest that cAMP functions downstream of ABA, modulating stress responses and contributing to enhanced resilience including in root tissues.

Phosphoproteomic analyses in tobacco cells have revealed that cAMP-dependent phosphorylation events have a central role in the reprogramming of gene expression during heat stress. Specific phosphorylation of RNA-binding proteins, transcription factors, and components of the translation machinery enables rapid and targeted adjustments in protein synthesis and stress signaling. This distinct phosphorylation footprint

points to a systemic regulatory role of cAMP in coordinating cellular adaptation to elevated temperatures [55].

Despite these advances, the precise mechanisms by which cAMP regulates the HSR remain incompletely understood. In this study, we investigate the role of intracellular cAMP in the HSR of *Arabidopsis thaliana* using two transgenic lines (cAS1 and cAS3). These lines overexpress a cAMP-sponge construct, which specifically sequesters 3',5'-cAMP [6, 7]. Particularly, previous RT- PCR analyses revealed the higher cAMP-sponge expression in the cAS3 line than in cAS1 line. Through physiological, ultrastructural, biochemical, and transcriptomic analyses, we aim to elucidate how cAMP contributes to the orchestration of the HSR and affects plant resilience to HS.

Materials and methods

Plant material

Arabidopsis thaliana overexpressing a “cAMP sponge” (cAS lines) based on the high-affinity cAMP-binding carboxy-terminus of the regulatory subunit of a protein kinase A were described by [1]. Seeds of WT Arabidopsis thaliana ecotype Columbia-0 [Col-0] wild-type (WT), cAS1 and cAS3 were surface sterilized using 70% ethanol (v/v) and 60% bleach (v/v) and then washed five times in sterile water. The seeds were sown on Murashige and Skoog (MS) plates supplemented with 2% sucrose and 1.5% plant agar. After stratification at 4°C for 2–3 days, plates were transferred to a growth chamber in basal condition of 22°C under long-day regime (16:8 h light/dark) and a light intensity of 120 µmol m–2s–1.

Heat stress treatment

WT and cAS seeds were sown on square plates, arranged in a single row at the top of the plate. The plants were grown vertically for 15 days at 22°C under long-day regime (16 hours of light/8 hours of dark). Heat stress was applied to 15-days-old seedlings by exposing plates to 45°C for 2 hours in dark conditions (Fig.9). Batches of control seedlings were maintained at 22°C. To allow short-term and long-term physiological recovery, plants were then incubated in growth conditions (22°C) for 3 hours or 2 days, respectively. Control plants were left at 22°C. The collected material was used to measure fresh weight and then frozen in liquid nitrogen and stored at -80 °C for later analysis.

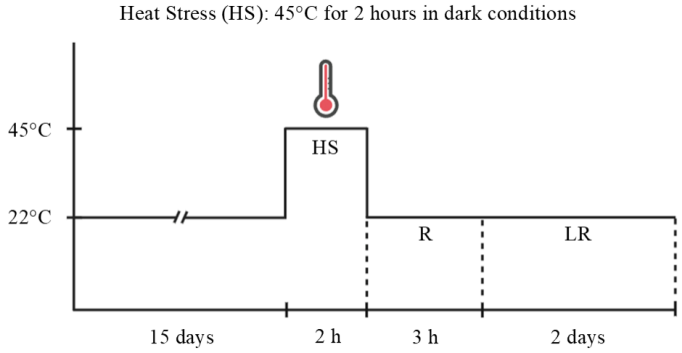

Figure 9. Schematic representation of the heat stress (HS) protocol.

Photosynthetic pigments quantification

About 50 mg of plant material were well ground into a homogeneous and fine powder by using a pre-cooled classical mortar and pestle in liquid nitrogen with 80% acetone (1:20 w/v). Samples were centrifuged at 20,000 x g for 20 min at 4°C. Absorbances were spectrophotometrically measured at wavelengths 470, 646.8 and 663.2 nm for carotenoids, chlorophyll b and chlorophyll a respectively [56]. Measures were performed in triplicate. Pigment concentrations were measured using the following equations [57]:

$$\text{Chl A} = 12{,}25 * A_{663.2} - 2{,}79 * A_{646.8}$$

$$\text{Chl B} = 21{,}50 * A_{646.8} - 5{,}10 * A_{663.2}$$

$$\text{Carotenoids} = (1000 * A_{470} - 1{,}82\ \text{Chl A} - 85{,}02 * \text{Chl B})/198$$

Transmission electron microscopy (TEM)

Leaf tissues from WT and cAS seedlings exposed to HS and long-recovery protocol (48 hours at 22°C) are fixed in 4% glutaraldehyde in 0.1 M cacodylate buffer (pH 7.4) for 1 h at room temperature, placed in a vacuum desiccator for 4 hours at room temperature and incubate overnight at 4 °C. Samples are rinsed twice with 0.1 M sodium cacodylate buffer for 10 min each, and post-fixation in 1% osmium tetroxide in 0.1 M cacodylate buffer for 2 hours at 4 °C. After two washes with double-distilled water (ddH_2O), samples are counterstained with 0.5% uranyl acetate in ddH_2O overnight at 4 °C in the dark. After rinsing with ddH2O, the tissues are dehydrated by subsequent immersions in increasing concentrations of ethanol for 10 min each. Subsequently, the samples are dehydrated twice with 100% ethanol for 15 min each. The tissues were then permeated twice with 100% propylene oxide for 15 min. The preparations are then transferred into propylene oxide and Epon resin (1:1 ratio) for 1 h, left overnight in resin and finally included. The semi-thin sections (0.75 µm) for light microscopy were cut with Reichert Ultracut S ultratome (Leica, Nussloch, Germany), collected on slides and coloured with crystal violet and basic fuchsine (Moore et al. 1960). The slides are observed with a Nikon Eclipse Ni light microscope (Nikon, Tokyo, Japan) and photographed with a Nikon Digital Sight DS-SM (Nikon, Tokyo, Japan) digital camera. Ultrathin sections (80 nm) are placed on copper grids, stained by uranyl acetate and lead citrate and observed with a Jeol 1010 EX transmission electron microscope TEM (Jeol, Tokyo, Japan). Data are recorded with a digital camera system (MORADA, Olympus, Tokyo, Japan).

cAMP extraction and quantification

Frozen WT and cAS3 plantlets were ground in liquid nitrogen in a 1,5 mL tube with pestles. The induction buffer (500 µM IBMX in PBS) was added to the samples, which were further homogenized mechanically. The homogenate was centrifuged (13 000 g x 15 min at 4°C). The supernatant was collected in a new tube and centrifuged a second time. The supernatant was splitted into two parts: one was refrigerated at -20°C as total cAMP fraction; the other one was further fractionated to separate free cAMP through a filter (Amicon Ultra-0,5 mL Centrifugal Filters, 10kDa cut-off). Free cAMP was measured in the extracts obtained with the Amicon Ultra-0.5 mL Centrifugal Filters (10-kDa cut-off) by the cAMPGlo™ assay kit (Promega, Madison, USA) and a microplate luminometer (Infinite M Plex Tecan, Switzerland) according to Promega's instructions.

NADPH oxidase activity

The NADPH oxidase-dependent generation of O2- in total membrane fractions of plant tissue has been determined by the reduction of the tetrazolium salt XTT by O_2^-. In the presence of O_2^-, XTT generates a soluble yellow formazan that can be quantified spectrophotometrically, as previously [58].

In membrane protein extractions, approximately 0.5 g of plant tissue was ground in liquid nitrogen using a pre-chilled mortar and pestle. If not processed immediately, the powder was stored at –80°C. The homogenized tissue was resuspended in 6 mL of ice-cold protein extraction buffer (1:12 w/v ratio; 0.25M surcrose, 50 mM, 4-(2-hydroxyethyl)-1-piperazineethanesulfonic acid (HEPES), 3mM Ethylenediaminetetraacetic acid (EDTA), 1 mM dithiothreitol (DTT), 3.6 mM L-cysteine, PVP-40 0.6%, PMSF 1 mM) and vortexed briefly at room temperature. The resulting homogenate was filtered through a paper filter. The flow-through was collected, transferred to 2 mL microcentrifuge tubes, and kept on ice. Samples were centrifuged at 10,000 × g for 45 minutes at 4°C, and the supernatant was carefully transferred to ultracentrifuge tubes (500 µL volume). Membrane fractions were then isolated by ultracentrifugation at 203,000 × g for 60 min at 4°C. The resulting supernatant was discarded, and the membrane-enriched pellet was resuspended in 200 µL of ice-cold 10 mM Tris-HCl buffer (pH 7.4). Protein estimation was performed

by using the Bradford microassay [59]. The NADPH-dependent O_2^- generating activity in the membrane fraction was determined after the reduction of XTT by O_2^-. The assay mixture contained 50 mM Tris-HCl buffer (pH 7.5), 0.5 mM XTT, 100 mM NADPH, and 20 µg of membrane proteins. XTT reduction was determined at 492 nm, at fixed time intervals of 5, 10, 15, and 30 minutes. Rates of O_2^- generation were calculated using an extinction coefficient of 2.16 × 104 $M_{-1}cm^{-1}$

The generation of superoxide anion (O_2^-) was quantified by measuring the absorbance at 492 nm at fixed time intervals of 5, 10, 15, and 30 minutes. Data analysis was performed by calculating O_2^- production using an extinction coefficient of $2.16 \times 10^4\ M^{-1}\ cm^{-1}$, as described elsewhere [60].

H_2O_2 visualization through 3,3′-diaminobenzidine (DAB) staining

In situ accumulation of H_2O_2 in leaves from WT, cAS1, and cAS3 seedlings subjected to the heat stress protocol was detected using 3,3'-diaminobenzidine (DAB) staining. Seedlings were vacuum-infiltrated (70–100 mbar) for 5 minutes with 100 mM phosphate buffer (pH 7.4) containing 0.1% (w/v) DAB. The seedlings were then incubated under vacuum in the dark for 5–6 h, until brown precipitates became visible. Subsequently, to remove chlorophyll, the stained seedlings were bleached with a series of washes in 95% ethanol at 45 °C. Staining intensity was quantified from digital images using ImageJ software (https://imagej.nih.gov/ij/) [61].

Determining ascorbate and glutathione levels in *A. thaliana*

To measure Ascorbate (ASC) and glutathione (GSH) content, approximately 0,3 g of pre-chilled plant material, collected in metaphosphoric acid 5% (v/v), was homogenized by vortexing. After centrifugation at 18,000 x g for 20 min at 4°C, the supernatant was collected.
Both ASC and dehydroascorbate (DHA) were quantified by adding 150 mM phosphate buffer (pH 7.4) and 5mM ethylenediaminetetraacetic acid (EDTA). To measure ASC, DHA was reduced by adding 10 mM dithiothreitol (DTT), and the samples were incubated for 10 min at room temperature to allow the reaction to proceed. To remove excess DTT, 50 µL of 0.5% N-ethylmaleimide (NEM) was added to the DHA samples. Subsequently, 10% trichloroacetic acid (TCA), 44% orthophosphoric acid, 4% 2,2'-dipyridyl (in 70% v/v ethanol), and 50 µL of iron (III) chloride (in 10% v/v TCA) were added to each sample, followed by incubation for 40 min at 40°C. The ASC concentration was determined spectrophotometrically (Beckman DU 7400) by measuring the absorbance at 525 nm. A conversion factor of 0.08666 was used which correspond to the absorbance of 1 µg/mL ASC. Results are expressed as nmol/g fresh weight (FW). DHA content was calculated as the difference between total ascorbate and ASC.
To measure the total amount of glutathione (GSH+ GSSG), 0,5mM phosphate buffer (pH 7.5) and H_2O were added to the supernatant. To measure the GSSG content, GSH was deactivated in the sample by adding the masking reagent 2-vinyl pyridine and incubated for 1h at room temperature.
The GSH content of the samples was calculated based on the enzymatic reaction:

$$2\ GSSG + NADPH + H^+ \rightleftarrows 2\ GSH + NADP^+$$

The reaction proceeded by mixing the sample extract (100 µL) in a reaction buffer (0,143 M potassium phosphate buffer containing 0,6 mM EDTA, pH 7.5), 5 mM 5,5′-dithiobis(2-nitrobenzoic acid) (DTNB). The reaction is initiated by adding 40 mM NADPH; after thorough mixing, the change in absorbance at 412 nm is measured upon the addition of 3 units of glutathione reductase (GR) and monitored for 60 seconds. The glutathione content was calculated using a conversion factor of 0.0406 nmol/µL.

Quantifying the enzymatic antioxidant activities in *A. thaliana* tissue

For quantifying the enzymatic antioxidant activities, 0.3 g of plant material wes ground in liquid nitrogen and homogenized with 4 volumes of extraction buffer (Tris-HCl 50 mM, pH 7.8, 0.05% cysteine (w/v), 0.1% bovine serum albumin (BSA) (w/v)). The homogenized samples were centrifuged at 20,000 x g for 15 min at 4°C. The protein amount was quantified using a Bradford assay.

Superoxide dismutase (SOD) activity was determined by adding PBS 100 mM (pH 7.8), ethylenediaminetetraacetic acid (EDTA) 0,1 mM, methionine 13 mM, nitroblue tetrazolium (NBT) 75 µM and riboflavin 0,5 mM to 10 µg of proteins. In parallel, a non-specific control series was prepared by replacing the extract with 50 µL of buffer and including riboflavin. After 15 minutes of exposure to white light the absorbance at 560 nm was measured.

The catalase (CAT) activity was determined by providing phosphate buffer 0.1 M (pH 7.0) to the sample extract (50-100 µg of protein). The reaction, carried out in a quartz cuvette, was initiated by adding H_2O_2 18 mM. Activity was measured as the decrease in absorbance at 240 nm due to H_2O_2 dismutation and expressed as nanomoles of H_2O_2 consumed per minute per milligram of protein, using a molar extinction coefficient of 23.5 mM^{-1} cm^{-1}.

Ascorbate peroxidase activity was determined by grinding approximately 0.1 g of plant material to a fine powder in liquid nitrogen using a mortar and pestle. Proteins were extracted by adding five volumes of extraction buffer containing 50 mM sodium phosphate (pH 7.0), 0.25 mM EDTA, 10% glycerol, and 1 mM freshly prepared ascorbate. The homogenate was centrifuged at 14,000 × *g* for 15 min at 4°C. The resulting supernatant was immediately used for spectrophotometric analysis to prevent decay of enzyme activity over time. Samples were prepared by adding the reaction mix (sodium-phosphate buffer 25mM, pH 7.0; EDTA 0.1 mM) to the supernatant. To initiate the enzymatic reaction, H_2O_2 (17 mM) and ascorbate (35 mM) were added to each sample. APX activity was calculated by monitoring the decrease in absorbance at 290 nm over 1 min, using a molar extinction coefficient of 2.7 mM^{-1} cm^{-1}.

RNA isolation, transcriptome sequencing and validation

Total RNA was extracted from 50–100 mg of frozen tissue of both WT and cAS3 seedlings with TriFast™ reagent (Trizol-based) according to the manufacturer's instructions. RNA integrity was monitored on 1% agarose gels ran at 100V for around 30 min; buffer used is TBE 0.5X (Tris Borato EDTA). RNA quality and quantity were examined by Nanodrop (TermoFisher Scientifics). The RNAseq was performed by the company. A total of 16 RNA samples were of sufficient quality on the basis of RIN value (RNA integrated number) calculated by using the Agilent 5400 Fragment Analyzer System. Sequencing was performed on the Illumina Hiseq X Ten platform.

RNA-seq raw counts from 16 samples, grouped into four conditions (CasS, CasC, WC, WS; n=4 biological replicate per condition), were processed using the edgeR package [62]. Before pairwise comparisons, we filtered out genes with very low expression, keeping only those with counts per million (CPM) > 0 in at least half of the samples. Then, we applied TMM (Trimmed Mean of M-values) normalization to adjust for differences in library size and composition. Principal Component Analysis (PCA) was performed using the prcomp function in base R to examine how the samples cluster based on their gene expression profiles. The first two principal components (PC1 and PC2) were scaled to a 0–100 range to improve visualization. The PCA plot was created using the ggplot2 package (for detail see reference [63]), where each experimental group is shown in a different colour, and sample names are added to help identify individual samples.

RNAseqChef, a comprehensive web application for automated, systematic, and integrated RNA-seq differential expression analysis [64] (https://imeg-ku.shinyapps.io/RNAseqChef/), was used to detect and visualize differentially expressed genes between conditions. For this, a multi-DEG analysis was performed, with DEGs identified using the DESeq2 R package, and an adjusted p-value (FDR < 0.05) using the Benjamini-Hochberg (BH) method. K-means clustering was then performed on the 8000 most significant genes, using a cluster number (k) of 8 and fold change cut-off 1.2. A heatmap of selected clusters was generated. For each cluster, a Gene Ontology (GO) enrichment analysis was performed using Shinygo 0.82 v.

In support of RNA-Seq results, quantitative real-time reverse transcription PCR (qRT-PCR) was performed. First-strand cDNAs were synthetized iScript cDNA Synthesis Kit (Biorad, Hercules, CA) based on three biological replicates. Quantitative real-time PCR reactions were performed with iTaq Univer SYBR Green (Biorad, Hercules, CA) in three technical replicates for each biological sample. The Actin2 (AT3G18780) and UBC21 (AT5G25760) were used as internal standard for HSP90 (At5g56030), LARP (At5g66100), HSF7B (At3g63350), LHCB (At1g03130), PSBO (At5g66570), while Ubiquitin10 (At4g05320) and Actin8 (At1g49240) were used as housekeeping genes for HSP101 (At1g74310.1), HSFA2 (At2g26150.1) and APX2 (At3g09640.1). The data analysis for relative quantification was perfomed as detailed elswhere [65]. The selected gene primers used in the qRT-PCR experiments are listed in Suppl. Table S1.

Results

Phenotypic characterization of plants subjected to heat stress

To investigate the role of cAMP in the heat stress (HS) response (HSR), 15-day-old wild-type (WT) and two transgenic Arabidopsis lines overexpressing a cAMP-sponge construct (cAS1 and cAS3) were subjected to 45°C for 2 hours, followed by recovery at 22°C for either 3 or 48 hours [66]. The phenotypical analysis showed that, after 2 days of recovery from HS (R-48h), cAS plants were significantly smaller than WT (Fig. 10A). The visible phenotype was confirmed by measuring whole plant fresh weight (Fig. 10B). Under control conditions, WT and cAS lines showed comparable growth, while after 48 hours of recovery from the HS cAS plants exhibited significantly reduced fresh weight compared to WT (Fig.10A-B), indicating impaired growth and biomass accumulation. This was accompanied by visible leaf chlorosis (Fig. 10A) and a marked reduction in photosynthetic pigments (Fig. 10C-E). Quantification of chlorophyll a and carotenoids showed a significant decline in cAS lines, particularly in cAS3, under recovery conditions (Figure 10C-E), suggesting compromised photosynthetic capacity.

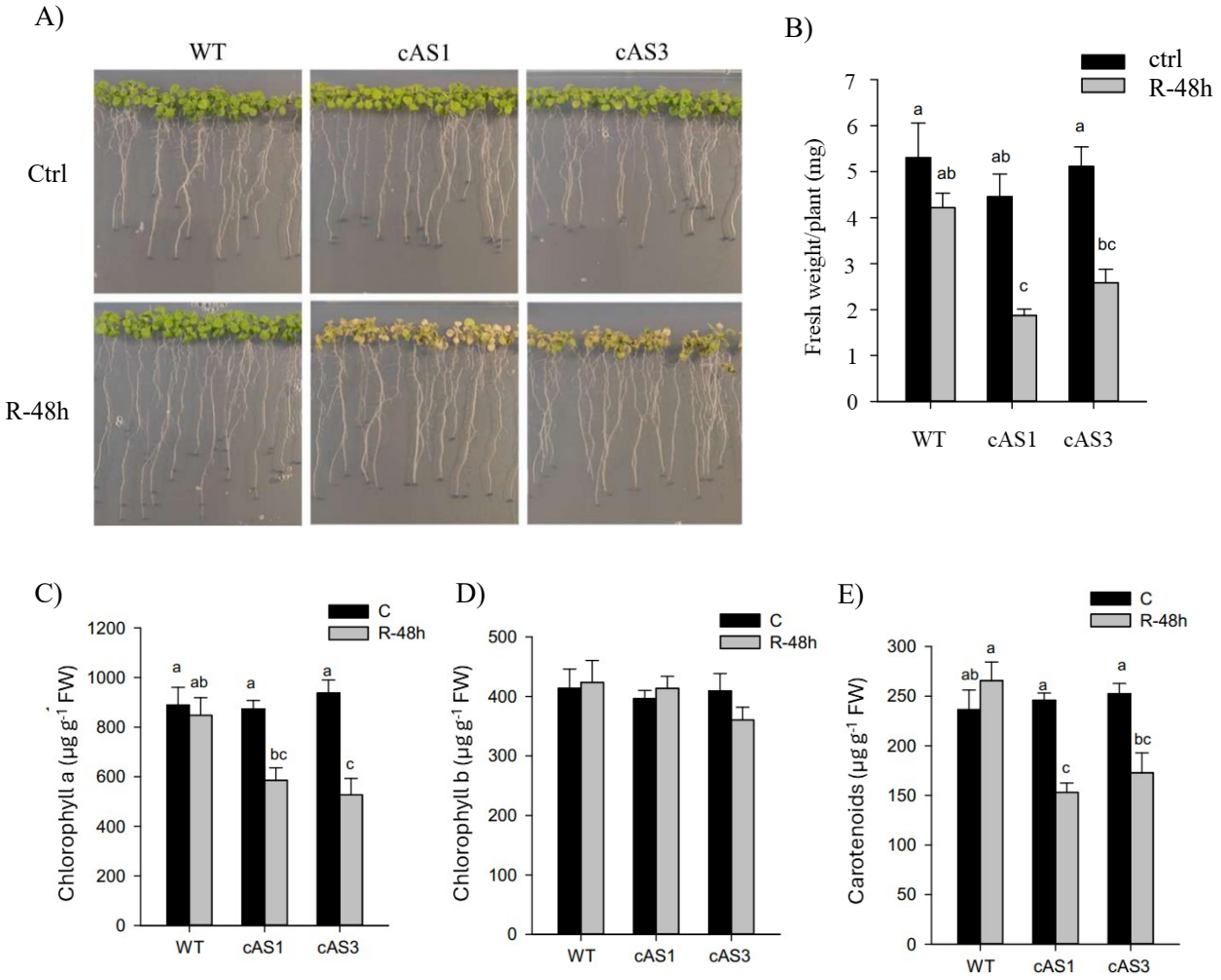

Fig.10 Representative image of visible phenotypes of WT, cAS1 and cAS3 after 2 days of recovery from the heat shock treatment (HS+LR). A) Leaf bleaching in plants subjected to stress and arrested root growth in plants exposed to the stress. Black lines were marked in both controls and stressed plants just before the stress. B) Fresh weight of plants subjected to HS+72h recovery. The values are the means ± standard error. Different letters indicate significant differences obtained by one-way ANOVA test ($P<0.05$). C) Changes in chlorophyll a, chlorophyll b, and carotenoids under HS treatments. Different letters indicate statistical differences in both control and after 48 h recovery (R-48h) conditions ($P<0.05$) according to the two-way ANOVA test.

Transmission electron microscope analysis on plants subjected to heat stress

Transmission electron microscopy images revealed pronounced structural damage in the chloroplasts of cAS plants following HS (Fig.12) compared to plants grown under control condition (Fig. 11). In WT plants, chloroplasts display well-organized grana stacks (Gr) and typical chloroplast features such as starch grains (St) and plastoglobules (Pg). In cAS lines, chloroplast ultrastructure is more severely disrupted, with evidence of disorganized grana stacking, an increased number or distorted appearance of plastoglobules and general signs of stress-related damage. These ultrastructural changes are consistent with impaired chloroplast function and stress adaptation.

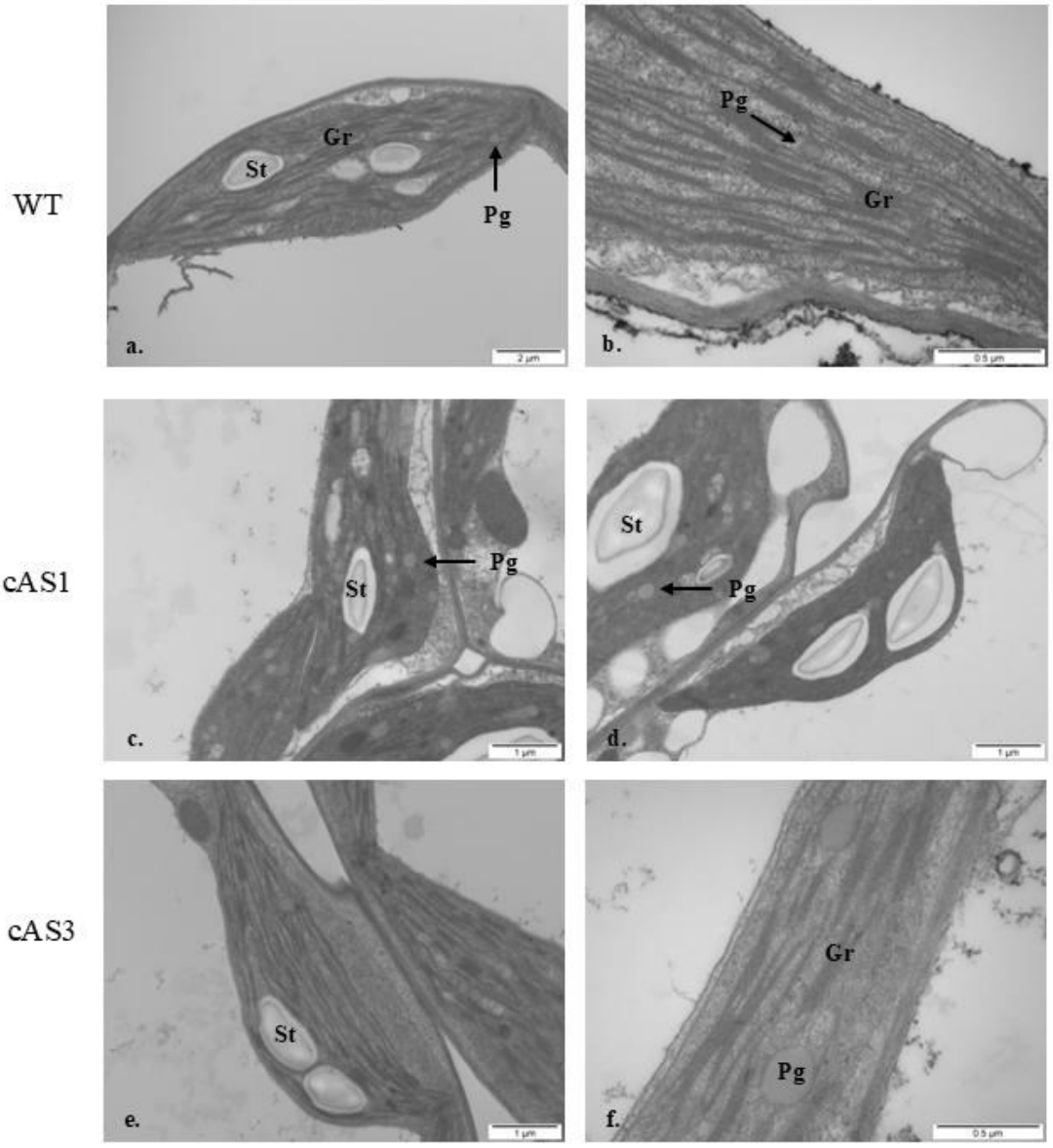

Figure 11. Transmission electron micrographs showing chloroplasts of plants under control conditions (22 °C). Gr, grana stacking; Mi, mitochondria; Pg, plastoglobules; St, starch grain.

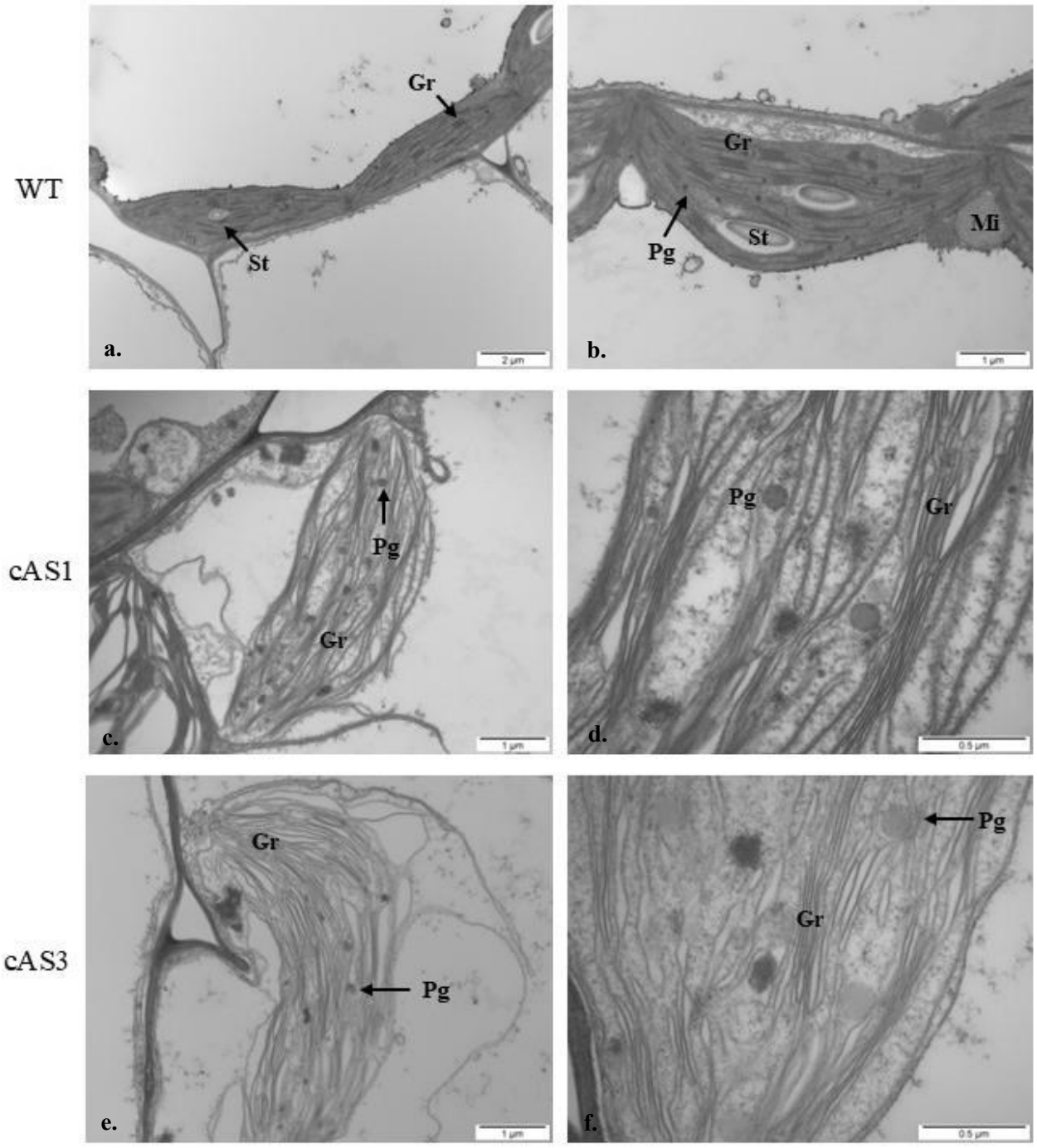

Figure 12. Transmission electron micrographs showing chloroplasts of plants subjected to HS (45 °C). Gr, grana stacking; Mi, mitochondria; Pg, plastoglobules; St, starch grain.

Free-cAMP levels in seedlings under heat stress and recovery

Under control conditions, free cAMP levels were lower in cAS3 plants overexpressing the cAMP sponge compared to WT, as previously reported [7]. The ratio of free cAMP under heat stress relative to control conditions (HS/C) was then used to assess changes in 3',5'-cAMP levels. In WT seedlings, cAMP levels increased by ~1.5-fold under heat stress, whereas no increase was detected in cAS3. This difference indicates a statistically significant genotype-dependent variation in the HS/C ratio. During recovery (R/C ratio), cAMP levels increased in cAS3 but remained unchanged in WT, suggesting that saturation of the cAMP sponge in cAS3 may lead to a delayed accumulation of free cAMP. Although not statistically significant, a tendency toward higher R/C values was observed in WT compared to cAS3, suggesting that the recovery trend remains lower in the cAS line (Fig. 13).

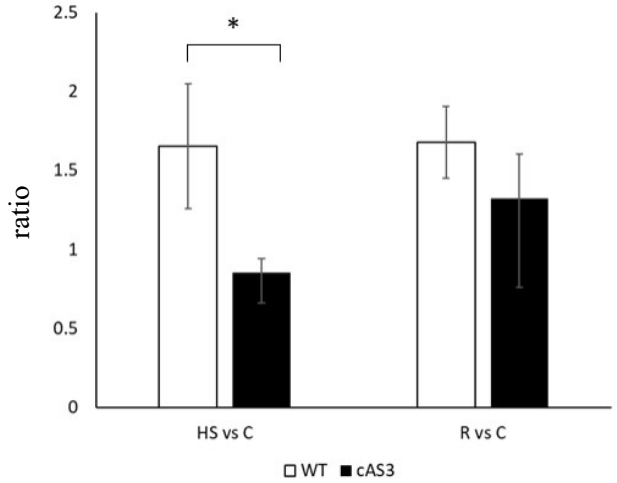

Figure 13. Free cAMP levels in WT and cAS3 seedlings under heat stress and recovery. Free cAMP was measured in 15-day-old seedlings grown under control conditions (C), subjected to heat stress (HS; 2 h at 45 °C), and after recovery (R; 3 h at 22 °C). Data are expressed as ratios (HS/C and R/C) ± SE from six biological replicates, each with two technical replicates. Asterisks indicate statistically significant differences ($p < 0.05$, Student's t-test), n=3 biological replicates.

Redox imbalance in cAMP-deficient Arabidopsis plants during the heat stress response

To evaluate ROS production and accumulation, NADPH oxidase activity and RBOHD (Respiratory Burst Oxidase Homolog D) expression, as well as hydrogen peroxide (H_2O_2) levels, were measured in WT and cAS Arabidopsis plants following HS and after a two-hour recovery period at 22°C (R). In WT plants, NADPH oxidase activity increased immediately after HS and returned to control levels in the R phase. In contrast, cAS plants exhibited a smaller increase in NADPH oxidase activity following HS; however, the activity continued to rise during the recovery (Figure 14A), suggesting enhanced ROS production.

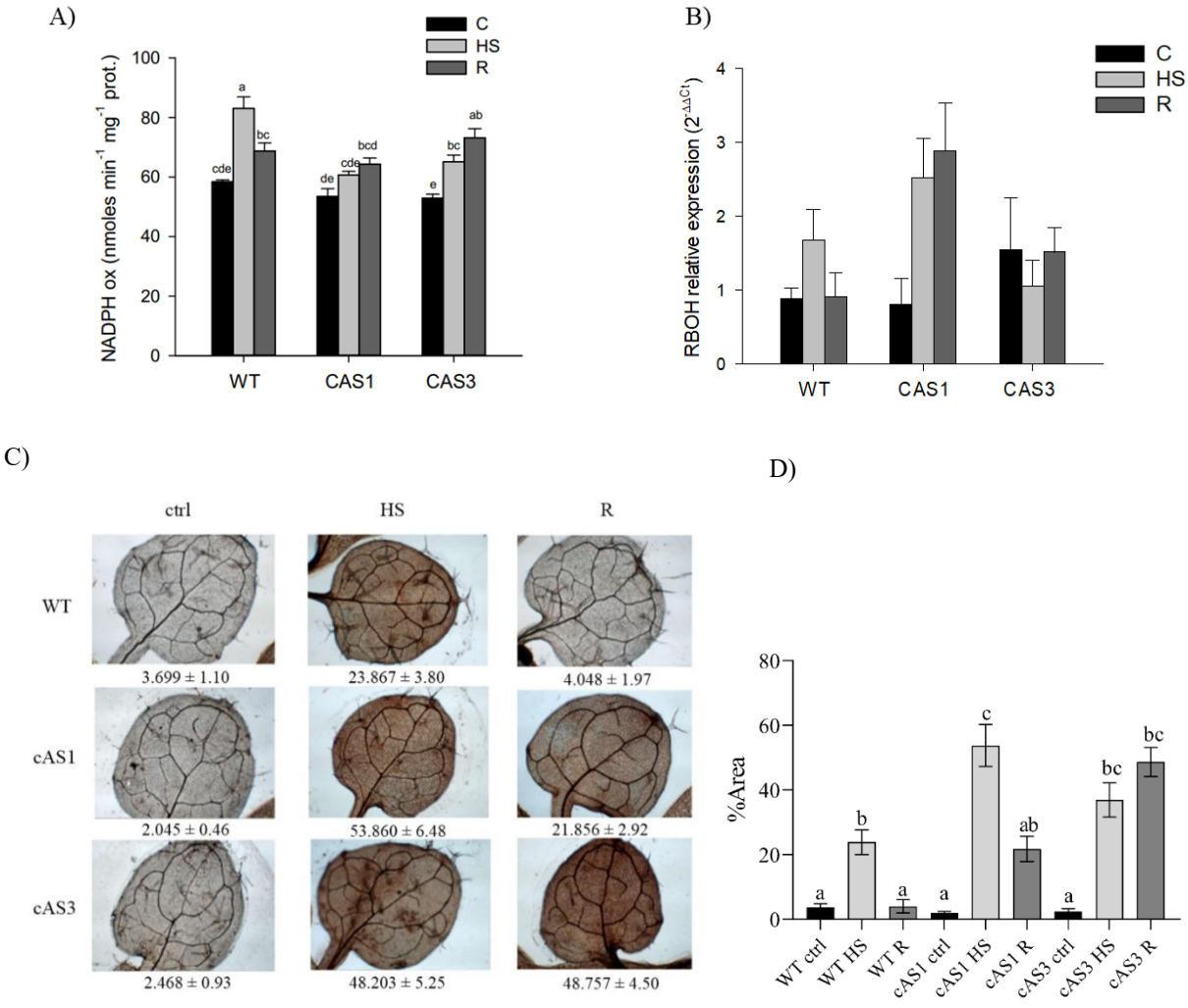

Figure 14. NADPH oxidase activity and accumulation of hydrogen peroxide (H_2O_2) in 15 days-old WT, cAS1 and cAS3 seedlings, grown at control temperature (C) or subjected to Heat Stress (HS; 2 hours at 45°C), followed by short recovery (R; 3 hours at 22°C). A) NADPH oxidase activity and B) RBOHD gene expression in WT, cAS1 and cAS3. Different letters indicate statistical differences between WT, cAS1 and cAS3 in each condition according to the two-way ANOVA test ($P<0.05$); C) Representative images of H_2O_2 accumulation, visualized by diaminobenzidine (DAB)-staining; D) H_2O_2 levels expressed as a %Area in WT and cAS3 plants under control (ctrl), heat stress (HS), and recovery (R) conditions. Different letters indicate statistical differences between WT, cAS1 and cAS3 in each condition according to the one-way ANOVA test ($P<0.05$).

The observed NADPH oxidase activity is corroborated by the expression patterns of the RBOHD gene. In WT Arabidopsis plants, RBOHD transcript levels exhibit a transient increase immediately following HS, returning to baseline levels during the recovery phase. This suggests a tightly regulated ROS production mechanism that supports stress signalling without prolonged oxidative damage. In contrast, both cAS lines show a sustained upregulation of RBOHD expression after HS, which persists throughout recovery. This prolonged activation may reflect a dysregulated redox response in cAMP-deficient plants, potentially contributing to excessive ROS accumulation (Fig. 14B).

DAB staining confirmed an increase in hydrogen peroxide (H_2O_2) accumulation in both WT and cAS Arabidopsis lines following HS. During the recovery phase, H_2O_2 levels returned to baseline in WT plants, whereas they remained elevated in the cAS lines, with the highest accumulation observed in cAS3 plants (Figure 14C-D).

The differential accumulation of H_2O_2 observed in WT and cAS Arabidopsis plants during the recovery phase following HS aligns with the distinct impacts of HS on their antioxidant defence systems (Figure 15). Under control conditions, the total levels of the two major hydrophilic antioxidants, ascorbate (ASC) and glutathione (GSH), did not differ significantly between WT and cAS plants (Figures 15A, B). In WT plants, ASC levels remained unchanged immediately after HS but increased significantly during the recovery phase. In contrast, cAS plants exhibited a less pronounced and statistically non-significant increase, suggesting a reduced capacity to mitigate oxidative stress (Figure 15A). Similarly, GSH content significantly increased in WT plants during recovery, whereas the response in cAS lines was attenuated and not statistically significant (Figure 15B).

To better understand the differential accumulation H_2O_2 in WT and cAS Arabidopsis plants during the HSR, the activities of key ROS-scavenging enzymes, superoxide dismutase (SOD), catalase (CAT), and ascorbate peroxidase (APX), were analyzed. Under control conditions, SOD activity was comparable in WT and cAS lines and remained largely unchanged following HS. However, a significant increase was observed during the recovery phase exclusively in WT plants (Figure 15C), pointing to a more effective post-stress antioxidant response. CAT activity in WT plants showed a transient decrease immediately after HS, followed by a marked increase during recovery. In contrast, the cAS lines exhibited a dampened CAT response, with no significant recovery-phase induction, indicating impaired H_2O_2 detoxification capacity (Figure 15D). APX activity was significantly higher in cAS lines than in WT under control conditions. Following HS, APX activity declined in all genotypes, with a more pronounced reduction in the cAS lines. During recovery, APX activity in WT plants rebounded to levels exceeding those observed under control conditions, whereas it remained low in both cAS lines (Figure 15E). These findings suggest that cAMP-deficient plants have a compromised ability to restore APX activity, contributing to sustained oxidative stress during recovery.

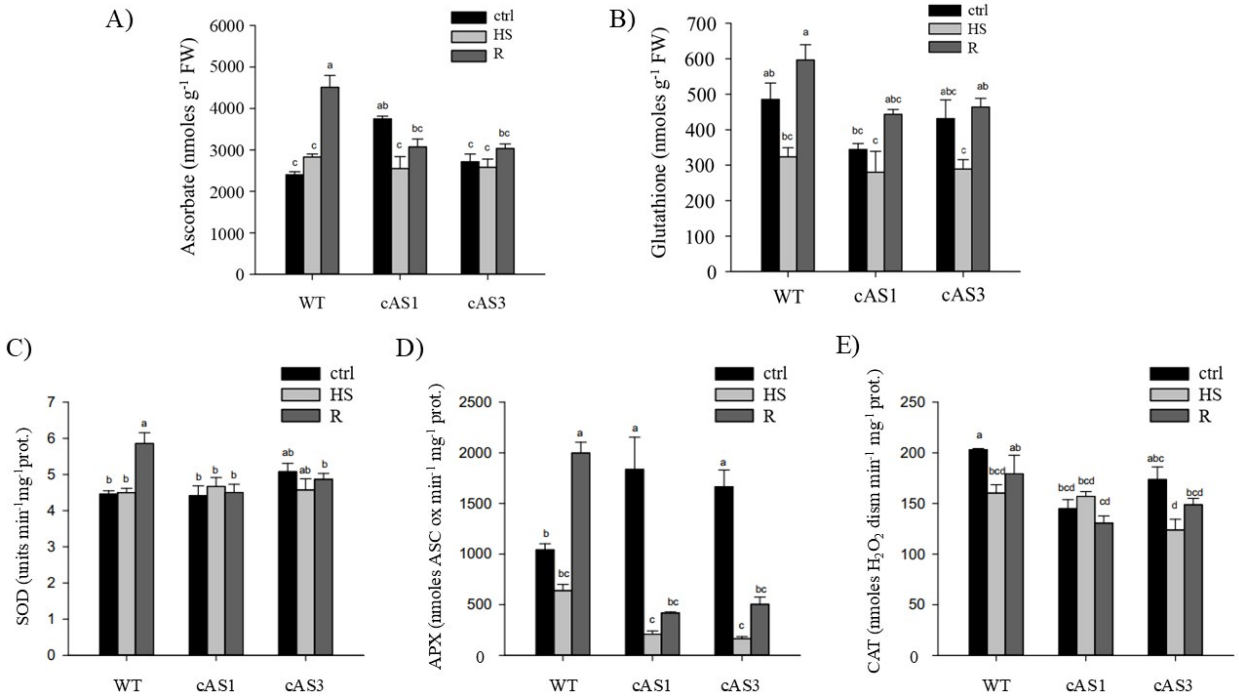

Figure 15. Non-enzymatic and enzymatic antioxidant of Arabidopsis WT and cAS lines, grown at control temperature (ctrl), subjected to heat stress (HS; 2 hours at 45°C), followed by short recovery (R; 3 hours at 22°C). A) Total ascorbate and B) glutathione contents; activities of C) superoxide dismutase (SOD), D) ascorbate peroxidase (APX) and E) catalase (CAT). The values are the means ± SE. Different letters indicate significant differences obtained by one-way ANOVA test ($p<0.05$), n= 3 biological replicates.

The transcriptome of cAMP-dependent basal thermotolerance in Arabidopsis

To investigate transcriptional events associated with cAMP-dependent basal thermotolerance, RNA-seq was performed on two-week-old WT and cAS seedlings under control conditions (22 °C) or following heat stress (2 h at 45 °C plus 3 h recovery at 22 °C). RNA from each treatment and genotype was sequenced in quadruplicate (Table S2). Principal component analysis (PCA) revealed that biological replicates clustered closely, indicating a good correlation between them (Fig. S1). The PCA plot showed a significant separation of control and heat-stressed samples along the first principal component (PC1), demonstrating that HS was the primary driver of transcriptional changes. Additionally, samples from wild-type (WT) and cAS plants exposed to heat stress were clearly separated, suggesting that genotype also had a noticeable influence on the transcriptome.

Analysis of the mapped reads revealed numerous differentially expressed genes (DEGs) across the treatments (Table S3). DEGs were clustered according to their expression profiles (Fig. 16).

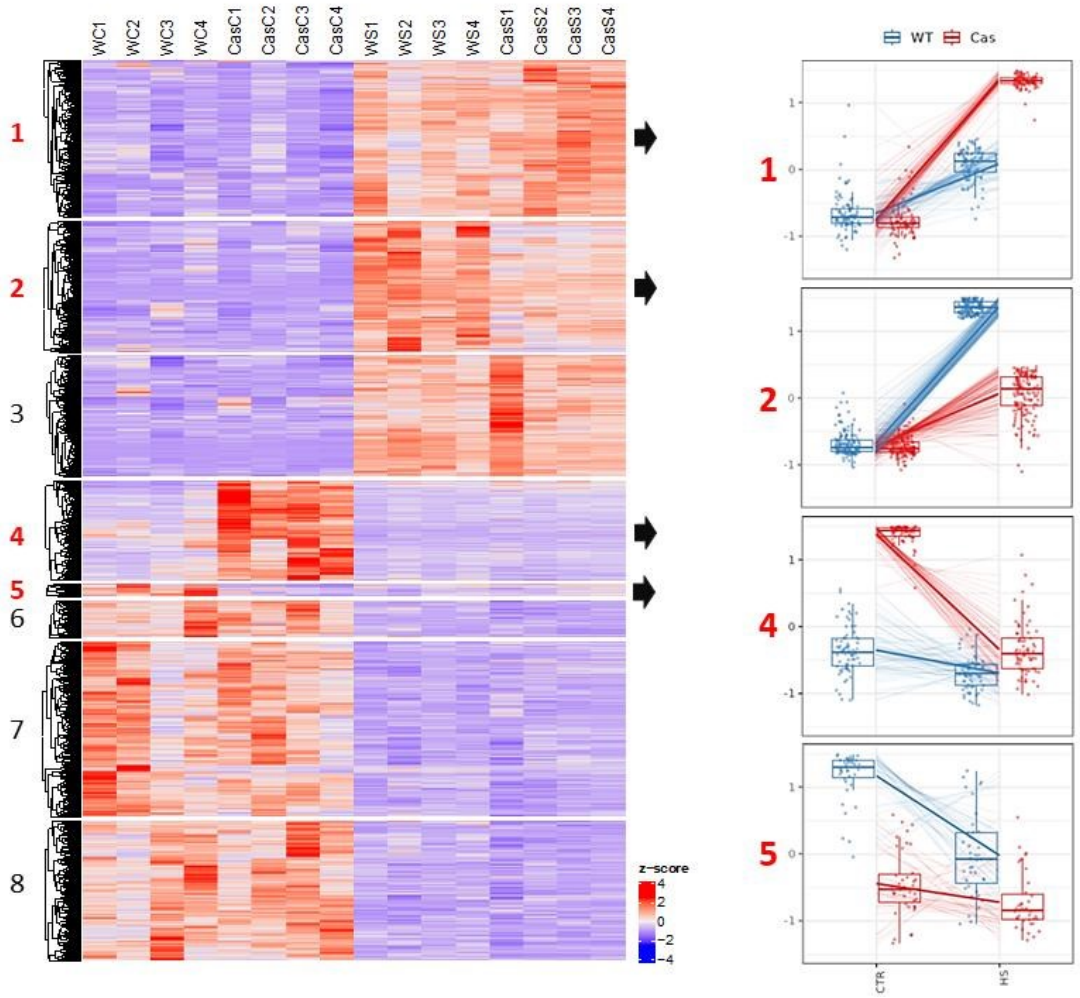

Figure 16. Gene clustering analysis for genes with altered expression upon HS.

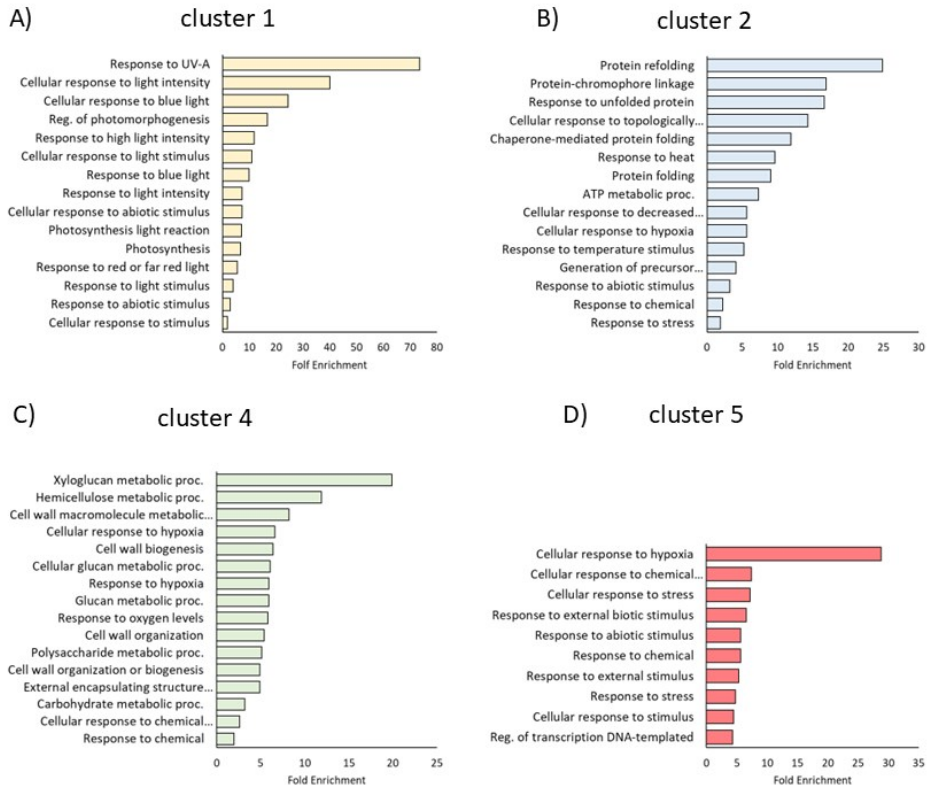

Figure 17. Biological Process enrichment of DEGs included in cluster 1(A), cluster 2(B), cluster 4 (C) and cluster 5 (D) by using ShinyGO V0.82 (based on Ensembl Release 104, Feb. 3, 2025) [67].

Among these, clusters 5 and 4 contained genes with consistent genotype-dependent expression, being more highly expressed in WT or cAS seedlings, respectively, under control conditions.

Gene Ontology (GO) enrichment of Cluster 5 indicated that cAMP damping alters stress responses and transcription regulator activity involved in early hormone signaling (Tables S10, S11). In particular, cAS seedlings displayed lower expression of multiple transcription factors (37% of DEGs) such as WRKY33 (WRKY DNA-binding protein 33), WRKY40 (WRKY DNA-binding protein 40), WRKY53 (WRKY DNA-binding protein 53), and WRKY70 (WRKY DNA-binding protein 70), together with ethylene-responsive regulators (ERF1, ERF2, and ERF104). Additional stress-related factors, including DREB1A (Dehydration-Responsive Element-Binding protein 1A), CBF1 (C-repeat Binding Factor 1), HSFA8 (Heat Shock Factor A8), and STZ (Salt Tolerance Zinc Finger), may point to a broad decrease of stress signaling pathways in cAS plants.
Cluster 4 (genes expressed in cAS) was enriched in biological processes related to cell wall biogenesis and organization including polysaccharide/hemicellulose/xyloglucan metabolism, along with responses to hypoxic stress and response to chemical stimulus. In this latter category we found several genes mediating the response to hormone stimulus such as three PYLs receptors A (tables S8, S9).

Notably, Clusters 1, 2, 3, 6, 7, and 8 are associated with the heat stress response (Figure 16, Tables S3). DEGs in Cluster 3 are upregulated during HS recovery in both genotypes, whereas DEGs of clusters 6, 7, and 8 are downregulated in both genotypes, representing a common response to HS recovery. To identify the cAMP-dependent responses to HS, we focused on clusters 2 and 1, which contain genes which responding to heat stress in a genotype-dependent manner.

Cluster 2 comprised genes expressed at higher levels in WT relative to cAS after recovery (tables S6, S7). GO analysis revealed enrichment in protein folding, chaperone-mediated refolding, and responses to heat and abiotic stress (Fig. 17B). In addition to multiple HSPs, notable genes included CLPB3 (AT5G15450), CLPB4 (AT2G25140), HSFA2 (AT2G26150), HSFB2B (AT4G11660), HSFA7B (AT3G63350), and APX2. Protein-chromophore linkage and ATP metabolism were also overrepresented biological processes. Enriched molecular functions included misfolded/unfolded protein binding, heat shock protein binding, electron transfer activity, NADH dehydrogenase activity, and chlorophyll binding. The corresponding cellular components were mitochondria, chloroplasts, and thylakoid membranes. KEGG (Kyoto Encyclopedia of Genes and Genomes) pathway analysis further highlighted the spliceosome as significantly overrepresented (table S7).

To gain further insights into functional relationships among cAMP-dependent DEGs, a high-confidence protein–protein interaction (PPI) network was constructed using STRING (Search Tool for the Retrieval of Interacting Genes/Proteins, https://string-db.org/) (Fig. 18). The majority of interacting DEGs were associated with protein folding, cellular response to heat, response to light intensity, mitochondrial membrane activity, and NADH dehydrogenase function. Additional clusters corresponded to disaccharide metabolism and ubiquitin-dependent protein catabolism. We proceeded to validate the shift observed in transcript levels by quantitative real-time PCR for some genes involved in the cAMP-dependent HS response.

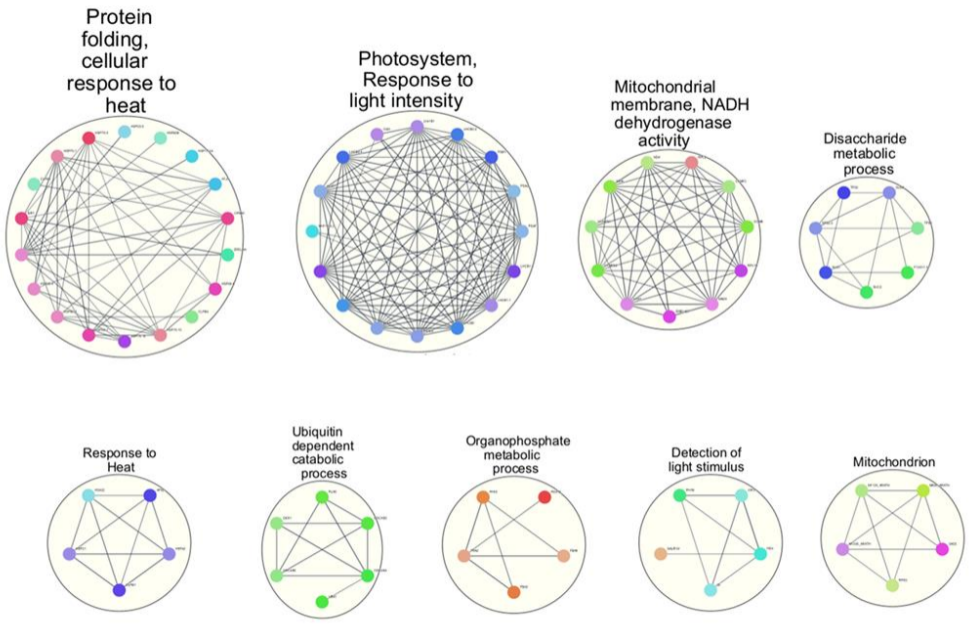

Figure 18. Functional protein-protein interaction networks of DAPs in cluster 2 by using STRING (version 12.0, https://string-db.org/cgi/input?sessionId=bC0Ep2I0fW6S&input_page_show_search=on).

The DEGs more expressed in cAS3 plants during HS recovery (cluster 1) provide information about the adaptive response elicited by plants with cAMP deficiency (tables S4,S5). GO analysis revealed that a significant activation of light and abiotic stress responses, including photosynthesis light reaction and regulation of photomorphogenesis. Consistently, cellular component analysis pointed to chloroplast-associated structures and molecular functions were enriched for transcriptional regulation and oxidoreductase activity. In particular, among these genes, tropinone reductases (At2g29290, At2g29320, At2g29370), a thiol-disulfide oxidoreductase (AT5G50100), two chloroplastic thioredoxin-like (AT1G07700, AT2G37240), a chloroplastic NADPH-dependent oxidoreductase (At1g23740), the glutathione peroxidases At4g31870, AT2G31570) were found.

Validation of transcriptomic analysis by qPCR

To validate RNA-seq results, quantitative real-time PCR was performed on selected genes of cluster 2. The transcriptomic trends were confirmed for all genes tested (Fig.19). Notably, HSP90 (At5g56030), LARP (At5g66100), LHCB (At1g03130) and PSBO (At5g66570) showed upregulation only after 3 h recovery. In contrast, the gene expression of HSF7B (At3g63350), HSP101 (At1g74310.1), HSFA2 (At2g26150.1), and APX2 (At3g09640.1) was induced by HS, however, this induction was lower in cAS3 line and the transcript numbers remained lower during recovery compared to WT.

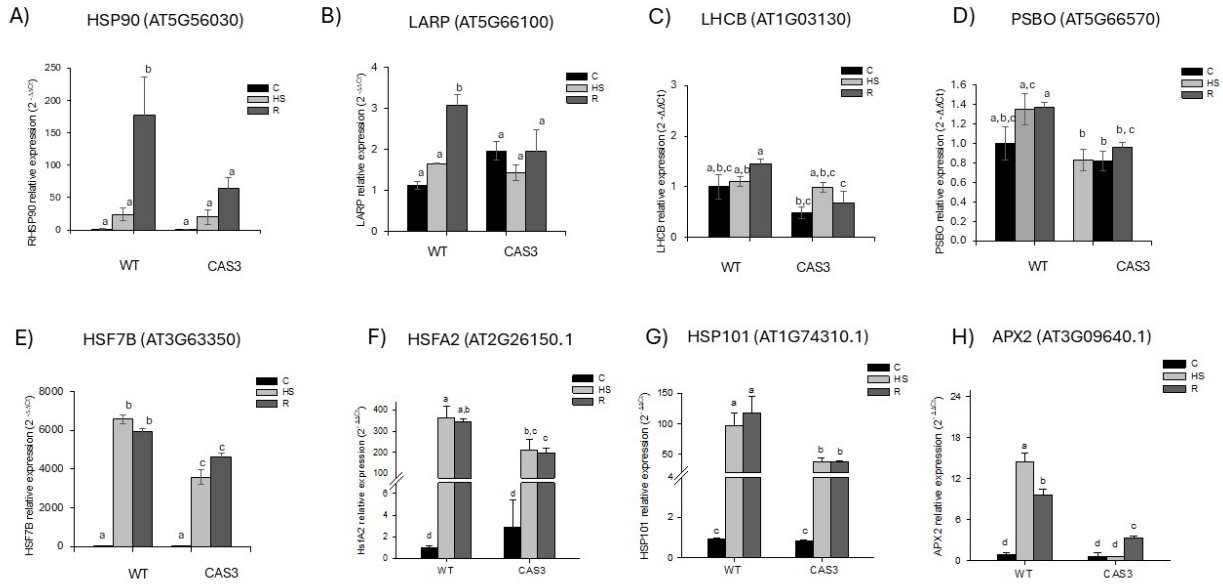

Figure 19. Expression level of HSP90 (AT5G56030) (A), LARP (AT5G66100) (B), LHCB (AT1G03130) (C), PSBO (AT5G66570) (D), HSF7B (AT3G63350) (E), HSFA2 (AT2G26150.1) (F), HSP101 (At1g74310.1) (G) and APX2 (AT3G09640.1) (H) in WT and cAS3 plants, collected after 2 h at 45°C (HS) and after 3 hours of recovery at 22°C (R). The expression level of HSP90, LARP, LHCB, PSBO and HSFA7B was normalized to that of Actin2 (AT3G18780) and UBC21 (AT5G25760); the expression level of HSFA2, HSP101 and APX2 was normalized to that of UBQ10 (AT4G05320) and ACT8 *(*AT1G49240). In each experiment, plants grown at 22°C were used as controls (C). Values are means (± SD) of three biological replicates (two technical replicates were included for each biological replicate). Statistical differences ($P < 0.05$) were obtained according to one way ANOVA test and different letters indicate significant differences.

Discussion

Cyclic adenosine monophosphate (cAMP) has been identified as a crucial secondary messenger in plant responses to both biotic and abiotic stress [7, 68–70]. In recent years, its role in the signaling pathways underlying heat stress response (HSR) has gained increasing attention [25, 29, 32, 37].

In *Arabidopsis thaliana*, mild heat shock triggers a rapid elevation in intracellular cAMP levels, which activates cyclic nucleotide-gated ion channel 6 (CNGC6). This activation facilitates a cytosolic influx of Ca^{2+}, initiating a cascade of downstream signalling events that promote the expression of heat-responsive genes and proteins [25, 71]. Similarly, in *Zea mays*, heat stress induces the expression of ZmRPP13-LK3, a putative disease-resistance protein with adenylate cyclase activity. The resulting increase in cAMP is proposed to contribute to abscisic acid-dependent thermotolerance mechanisms [29]. In tobacco BY-2 cells, prolonged heat exposure also leads to cAMP accumulation, which is essential for maintaining thermotolerance. In transgenic tobacco cells overexpressing a cAMP-sponge construct, that specifically buffers cAMP levels, the heat-induced rise in cAMP is suppressed. This deficiency correlates with increased sensitivity to heat stress, manifested by elevated cell death and reduced accumulation of proteins associated with the ubiquitin-proteasome system [37]. Exogenous application of cAMP restores cell viability in cAS tobacco cells and improves thermotolerance in Arabidopsis treated with cAMP analogues [25, 37].

Experimental data from this study further support the involvement of cAMP in HSR. In Arabidpopsis, the increase of cAMP in response to HS is significantly reduced in plants overexpressing the cAMP sponge (cAS 3 line; Fig.13). Moreover, Arabidopsis lines overexpressing the cAMP sponge (cAS1 and cAS3) display increased sensitivity to heat stress, as evidenced by reduced growth and chlorosis, which correlate with diminished levels of chlorophyll a and carotenoids (Fig. 10). Under heat stress conditions, an elevated chlorophyll a/chlorophyll b (Chl a/Chl b) ratio is commonly associated with the selective degradation of light-harvesting complex II proteins, which serves as a photoprotective strategy to reduce excitation pressure on system II (PSII) [72]. In tomato, a higher Chl a/Chl b ratio has been positively correlated with enhanced thermotolerance [73]. In the present study, *Arabidopsis thaliana* cAMP-sponge (cAS) lines exhibited a reduction in Chl a levels without a corresponding decline in Chl b at two days post-recovery (Fig. 10), resulting in a decreased Chl a/Chl b ratio. This imbalance suggests a compromised ability to implement photoprotective mechanisms, thereby impairing the resilience of the photosynthetic apparatus under heat stress conditions. These results relate with the changes in chloroplast ultrastructure induced by heat stress. Transmission electron microscopy (TEM) analyses indicated that chloroplasts of cAS3 line experienced more severe damage from heat stress compared to those in WT plants (Fig. 12). Photosystem II (PSII) is recognized as one of the most heat-sensitive components within the photosynthetic apparatus. Its susceptibility to heat stress is primarily attributed to two key factors: the increased fluidity of thylakoid membranes at elevated temperatures, which can lead to the displacement of PSII light-harvesting complexes from the membrane and, the reliance of PSII integrity on the dynamics of electron transport. This suggests that in cAS lines, alterations in chloroplast integrity may contribute to their lower photosynthetic efficiency and resilience under heat stress conditions [74]. Additionally, heat stress can compromise the integrity of thylakoid membranes, affecting ion conductivity and phosphorylation activity. Exposure to elevated temperatures can induce the destacking of grana, thereby impairing the proper functioning of the photosynthetic apparatus [75]. Damage to the photosynthetic apparatus under heat stress conditions can lead to elevated production of ROS, resulting in their intracellular accumulation and the onset of oxidative stress. Consistent with this, after three hours of recovery from heat stress, Arabidopsis cAS plants exhibited significantly higher levels of hydrogen peroxide (H_2O_2) compared to WT plants (Fig.14).

In WT plants, heat stress triggered a rapid and transient increase in H_2O_2 levels, which was accompanied by a parallel rise in NADPH oxidase activity immediately following exposure. Notably, both H_2O_2 and NADPH oxidase activity returned to baseline levels comparable to control conditions within three hours of recovery (Fig.14). In wild-type WT plants, the transient HS - induced oxidative burst appears to be a tightly regulated event that contributes to redox signalling pathways essential for activating protective and adaptive mechanisms during the HSR [66, 76]. The regulation of antioxidant enzyme activity is closely associated with the development of thermotolerance in plants [39]. Heat stress (HS) can transiently suppress the activity of ROS-detoxifying enzymes, allowing for a controlled oxidative burst that functions as a redox

signal to activate heat-responsive gene expression [39, 66]. In WT plants, the activity of ascorbate peroxidase (APX) was reduced immediately following HS but significantly increased during the recovery phase. Similarly, superoxide dismutase (SOD) activity was elevated during recovery, indicating a coordinated antioxidant response (Fig.15C).

In contrast to WT plants, cAMP-deficient Arabidopsis lines failed to restore the activity of key antioxidant enzymes (APX and SOD) after three hours of recovery from heat stress (HS) (Fig. 10D-E), resulting in sustained oxidative stress. These findings are consistent with previous observations in tobacco cAMP-sponge (cAS) cells, where the inability to upregulate catalase and APX under HS conditions led to excessive accumulation of ROS [37].

The cAMP-dependent upregulation of the enzymatic ROS-scavengers (APX and SOD), with consequent reduced H_2O_2 levels and oxidative damage, has been observed in *Zea mays* plants, pre-treated with the cAMP analogue 8-Br-cAMP before HS [29]. In contrast, pharmacological inhibition of adenylate cyclase resulted in elevated oxidative markers, reinforcing the critical role of cAMP in regulating antioxidant defense mechanisms under heat stress conditions [29]. In Arabidopsis cAS plants, the impaired activation of enzymatic antioxidants was accompanied by a significant reduction in non-enzymatic antioxidants, specifically ascorbate (ASC) and glutathione (GSH), throughout the recovery phase (Fig.15A-B). This dual deficiency exacerbated intracellular ROS accumulation, compromising plant's ability to mitigate oxidative damage and restore redox balance.

Transcriptomic analysis of WT and cAS plants grown at 22 °C provided insights into how cAMP damping affects native cAMP signalling. cAS plants exhibited reduced expression of several transcription factors associated with stress responses and hormone signalling, including those regulated by abscisic acid (ABA), ethylene, jasmonic acid, and salicylic acid. By contrast, genes overexpressed in cAS plants relative to WT were associated mainly with cell wall organization or biogenesis, and response to stimulus.

Remarkably, about 30% of these DEGs have previously been reported as repressed by endogenous cAMP elevation in Arabidopsis ([77], Fig. S2), supporting the idea that reduced cAMP level promote their expression.

The upregulation of genes such as pectin lyases, arabinogalactan proteins, xyloglucan endotransglucosylase/hydrolases, pectinesterases, and expansins suggests enhanced cell wall loosening and expansion. Beyond serving as the first physical barrier against heat stress, the cell wall actively participates in the heat stress response (HSR) through signaling pathways [78]. Thus, cell wall remodeling in cAS plants may directly affect heat stress perception and/or signal transduction. Within the category "response to stimulus", we identified genes coding for proteins involved in the signaling of cytokinin, auxin, brassinosteroids, and abscisic acid (ABA). Notably, this group included EAR1 (AT5G22090) and FERONIA (AT3G51550), two well-characterized negative regulators of ABA signaling [79, 80].

The HSR integrates multiple phytohormone pathways, among which ABA response pathway may have a central role. For example, Arabidopsis mutants deficient in ABA biosynthesis or signaling display impaired basal and acquired thermotolerance. Consistently, our transcriptomic data revealed that the gene encoding NCED3, a key enzyme in ABA biosynthesis, was more strongly expressed in WT plants than in cAS3 during HS recovery. Interestingly, NCED3 has also been identified as an adenylate cyclase, and its overexpression elevates both ABA and cAMP levels, thereby amplifying ABA signaling.

Taken together, these findings indicate that cAMP levels modulate phytohormone signalling, biotic and abiotic stress responses, and plant growth and development. They are consistent with previous reports in Arabidopsis and Brassica [77, 81], reinforcing the view that tight regulation of intracellular cAMP concentrations is essential for maintaining the balance between stress adaptation and plant growth.

Quantification of free cAMP indicated that, although both WT and cAS3 showed increased cAMP during heat stress and recovery, the rise was markedly attenuated in cAS3.

This reduced availability of cAMP can led to incomplete activation of the HSR, as evidenced by cluster 2 genes, which were significantly more expressed in WT than in cAS3. Time-course expression analysis of some heat marker genes (HSP101, APX2, HSFA2, and HSFA7B) confirmed higher transcript levels in WT plants after heat stress, with differences maintained during recovery.

Among cAMP-dependent heat-responsive genes, several encode chaperones that mitigate misfolded protein accumulation in the cytosol and organelles. Particularly noteworthy are HSP21 and CLPB3. HSP21 is a key chloroplast chaperone that preserves thylakoid membrane integrity under heat stress. Its expression depends on the GUN5-mediated retrograde signaling pathway (Genomes Uncoupled 5), and HSP21 (Heat Shock Protein 21) directly binds PSII subunits, stabilizing them to prevent or minimize thermal damage [82]. Under HS, protein aggregates accumulate in the chloroplast; a retrograde signaling pathway, known as the chloroplast unfolded protein response, is activated, leading to the transcription of nuclear genes that encode plastidial chaperones such as CLPB3 (Casein Lytic Proteinase B3), which disassemble protein aggregates.

The concomitant reduction of GUN5, HSP21, and CLBP3 expression in cAS plants suggests that cAMP interferes with the chloroplast–nucleus communication, which is essential for activating nuclear genes involved in stress adaptation. In particular, the attenuated expression of HSP21 may explain the greater chloroplast vulnerability observed at the ultrastructural level in cAS plants, characterized by thylakoid membrane damage and grana disorganization.

In contrast, WT plants upregulate several genes involved in photosystem I and II subunit biosynthesis and chlorophyll production, supporting the idea that their ability to repair and restore photosynthetic efficiency after heat stress might be essential. This transcriptional response is consistent with the recovery of chlorophyll and carotenoid levels observed in WT seedlings. Heat-responsive transcription factors also contribute to these differences. HSFA2 (Heat Shock Factor A2) has a central role in cytosolic responses to misfolded proteins. At the same time, HSFA7B (Heat Shock Factor A 7B) regulates ethylene biosynthesis and signaling, thereby contributing to thermomemory at the shoot apical meristem, for example, controlling the maintenance of the shoot apical meristem stem cell pool [83].

After three hours of recovery, transcripts encoding respiratory proteins and mitochondrial functions were also more abundant in WT than in cAS3. For example, NDB2, which catalyzes the majority of exogenous NADH oxidation in mitochondria, is required for the recovery from environmental stress and was upregulated in WT but not in cAS3. These molecular signatures are consistent with the more pronounced post-stress growth recovery observed in WT plants [84].

In contrast, the impairment of chloroplast and mitochondrial functions in cAS plants likely contributed to excessive ROS accumulation after heat stress, as indicated by the DAB staining (Fig. 14C). The redox imbalance in cAS3 was further supported by expression profiles in cluster 1, which included genes encoding ROS detoxification enzymes such as glutathione peroxidases, alcohol oxidoreductase, which detoxifies carbonyl groups from lipid peroxidation, and short-chain dehydrogenase/reductase, also involved in carbonyl detoxification. Additionally, mitochondrial thiol-disulfide reductases were activated in cAS3, likely as a compensatory response to mitochondrial redox imbalance. However, this activation is a marker of prolonged stress and reflects the failure of cAS plants to properly overcome the oxidative stress during the recovery phase.

In cluster 3, where heat-induced transcriptional activation occurs similarly in both WT and cAS3 genotypes, the transcription factor HSFA1b emerges as a key regulator of the HSR. Notably, HSFA1b exhibits a dual function: beyond its canonical role as a heat-responsive transcription factor, it also functions as an adenylate cyclase, directly contributing to intracellular cAMP production.

Through its adenylate cyclase activity, HSFA1b was proposed to modulate OST1 (Open Stomata 1), a critical kinase in ABA and stress signaling pathways [85]. This may interaction underscores an expanded role of HSFA1b, not only in transcriptional regulation but also in post-translational control of signaling kinases, thereby strengthening its importance as a thermosensitive hub in plant stress responses.

While this regulatory mechanism is conserved in both genotypes, indicating that initial HSR activation remains intact in cAS3, the downstream efficiency of the heat stress response diverges in cAS3 line. This divergence is likely due to disrupted cAMP homeostasis and signaling caused by the action of the cAMP-sponge, which is likely to compromise the sustained enabling of the stress responses e.g. through effects on hormone signaling or other cAMP-dependent pathways. cAS3 plants exhibit lower levels of free cAMP even under non-stress conditions, suggesting a pre-existing alteration in signaling that becomes more pronounced under heat stress.

Conclusions

The findings presented in this chapter highlight the central role of cAMP-mediated signaling in orchestrating the plant's adaptative response to heat stress. cAMP emerges as a dynamic regulator that integrates multiple layers of cellular activity, ranging from transcriptional reprogramming to redox homeostasis and organelle function.

Through the use of the cAS lines, in which intracellular cAMP levels are artificially buffered by a sponge construct, we were able to dissect the consequences of impaired cAMP signalling. Plants expressing the cAMP-sponge altering the cAMP dynamics, exhibit a markedly compromised heat stress response, characterized by attenuated activation of canonical HSR genes and antioxidant defenses, and impaired functionality of key organelles such as mitochondria and chloroplasts. These alterations translate into visible physiological consequences, including structural damage and sustained oxidative stress during the recovery phase, following heat exposure.

Taken together, these findings support a model in which cAMP serves not just as a secondary messenger, but as a master regulator of stress resilience. By modulating gene expression, redox balance, and organelle performance, cAMP ensures that plants can promptly and effectively respond to elevated temperatures.

Bibliography

1. Świeżawska B, Duszyn M, Jaworski K, Szmidt-Jaworska A. Downstream targets of cyclic nucleotides in plants. Frontiers in Plant Science. 2018;9 October:1–7. https://doi.org/10.3389/fpls.2018.01428.

2. Gehring C, Turek IS. Cyclic nucleotide monophosphates and their cyclases in plant signaling. Frontiers in Plant Science. 2017;8 October:1–15. https://doi.org/10.3389/fpls.2017.01704.

3. Rall Tw, Sutherland Ew. Formation Of A Cyclic Adenine Ribonucleotide By Tissue Particles. Journal Of Biological Chemistry. 1958;232:1065–76. Https://Doi.Org/10.1016/S0021-9258(19)77422-5.

4. Makman Rs, Sutherland Ew. Adenosine 3‘,5‘-Phosphate in Escherichia coli. Journal of Biological Chemistry. 1965;240:1309–14. https://doi.org/10.1016/S0021-9258(18)97576-9.

5. Sy J, Richter D. Separation of a cyclic 3’, 5’-adenosine monophosphate binding protein from yeast. Biochemistry. 1972;11:2784–7.

6. Sabetta W, Vannini C, Sgobba A, Marsoni M, Paradiso A, Ortolani F, et al. Cyclic AMP deficiency negatively affects cell growth and enhances stress-related responses in tobacco Bright Yellow-2 cells. Plant Molecular Biology. 2016;90:467–83. https://doi.org/10.1007/s11103-016-0431-5.

7. Sabetta W, Vandelle E, Locato V, Costa A, Cimini S, Bittencourt Moura A, et al. Genetic buffering of cyclic AMP in Arabidopsis thaliana compromises the plant immune response triggered by an avirulent strain of Pseudomonas syringae pv. tomato. Plant Journal. 2019;98:590–606. https://doi.org/10.1111/tpj.14275.

8. Kwiatkowski M, Zhang J, Zhou W, Gehring C, Wong A. Cyclic nucleotides – the rise of a family. Trends in Plant Science. 2024;29:915–24. https://doi.org/10.1016/j.tplants.2024.02.003.

9. Li W, Luan S, Schreiber SL, Assmann SM. Cyclic AMP stimulates K+ channel activity in mesophyll cells of Vicia faba L. Plant Physiology. 1994;106:957–61. https://doi.org/10.1104/pp.106.3.957.

10. Figueroa NE, Franz P, Luzarowski M, Martinez-Seidel F, Moreno JC, Childs D, et al. Protein interactome of 3′,5′-cAMP reveals its role in regulating the actin cytoskeleton. Plant Journal. 2023;115:1214–30. https://doi.org/10.1111/tpj.16313.

11. Van Damme T, Blancquaert D, Couturon P, Van Der Straeten D, Sandra P, Lynen F. Wounding stress causes rapid increase in concentration of the naturally occurring 2′,3′-isomers of cyclic guanosine- and cyclic adenosine monophosphate (cGMP and cAMP) in plant tissues. Phytochemistry. 2014;103:59–66. https://doi.org/10.1016/j.phytochem.2014.03.013.

12. Moutinho A, Hussey PJ, Trewavas AJ, Malhó R. cAMP acts as a second messenger in pollen tube growth and reorientation. Proceedings of the National Academy of Sciences. 2001;98:10481–6. https://doi.org/10.1073/pnas.171104598.

13. Gehring C. Adenyl cyclases and cAMP in plant signaling - Past and present. Cell Communication and Signaling. 2010;8:1–5. https://doi.org/10.1186/1478-811X-8-15.

14. Ruzvidzo O, Gehring C, Wong A. New Perspectives on Plant Adenylyl Cyclases. Frontiers in Molecular Biosciences. 2019;6 December:1–8. https://doi.org/10.3389/fmolb.2019.00136.

15. Fortunato S, Domingo G, Davide E, Lasorella C, Bracale M, Vannini C, et al. Dual function plant cryptic nucleotide cyclases. Cryptic Enzymes and Moonlighting Proteins. 2025;:135–72. https://doi.org/10.1016/B978-0-443-15719-6.00007-6.

16. Turek I, Irving H. Moonlighting proteins shine new light on molecular signaling niches. International Journal of Molecular Sciences. 2021;22:1–22. https://doi.org/10.3390/ijms22031367.

17. Al-younis I, Wong A, Gehring C, Wong A. Functional Crypto-Adenylate Cyclases Operate in Complex Plant Proteins. 2021;12 August. https://doi.org/10.3389/fpls.2021.711749.

18. Al-Younis I, Wong A, Lemtiri-Chlieh F, Schmöckel S, Tester M, Gehring C, et al. The arabidopsis thaliana K+ -uptake permease 5 (AtKUP5) contains a functional cytosolic adenylate cyclase essential for

K+ transport. Frontiers in Plant Science. 2018;871 November:1–15. https://doi.org/10.3389/fpls.2018.01645.

19. Kwiatkowski M, Wong A, Kozakiewicz A, Gehring C, Jaworski K. A tandem motif-based and structural approach can identify hidden functional phosphodiesterases. Computational and Structural Biotechnology Journal. 2021;19:970–5. https://doi.org/10.1016/j.csbj.2021.01.036.

20. Fortunato S, Domingo G, Davide E, Lasorella C, Bracale M, Vannini C, et al. Chapter 7 - Dual function plant cryptic nucleotide cyclases. In: Irving H, Gehring C, Wong ABT-CE and MP, editors. Foundations and Frontiers in Enzymology. Academic Press; 2025. p. 135–72. https://doi.org/https://doi.org/10.1016/B978-0-443-15719-6.00007-6.

21. Blanco E, Fortunato S, Viggiano L, de Pinto MC. Cyclic amp: A polyhedral signalling molecule in plants. International Journal of Molecular Sciences. 2020;21:1–2. https://doi.org/10.3390/ijms21144862.

22. Yang Y, Tan YQ, Wang X, Li JJ, Du BY, Zhu M, et al. OPEN STOMATA 1 phosphorylates CYCLIC NUCLEOTIDE-GATED CHANNELs to trigger Ca2+ signaling for abscisic acid-induced stomatal closure in Arabidopsis. Plant Cell. 2024;36:2328–58. https://doi.org/10.1093/plcell/koae073.

23. Qi L, Kwiatkowski M, Chen H, Hoermayer L, Sinclair S, Zou M, et al. Adenylate cyclase activity of TIR1/AFB auxin receptors in plants. Nature. 2022;611:133–8. https://doi.org/10.1038/s41586-022-05369-7.

24. Qi L, Friml J. Tale of cAMP as a second messenger in auxin signaling and beyond. New Phytologist. 2023;240:489–95. https://doi.org/10.1111/nph.19123.

25. Gao F, Han X, Wu J, Zheng S, Shang Z, Sun D, et al. A heat-activated calcium-permeable channel - Arabidopsis cyclic nucleotide-gated ion channel 6 - Is involved in heat shock responses. Plant Journal. 2012;70:1056–69. https://doi.org/10.1111/j.1365-313X.2012.04969.x.

26. Donaldson L, Ludidi N, Knight MR, Gehring C, Denby K. Salt and osmotic stress cause rapid increases in Arabidopsis thaliana cGMP levels. FEBS Letters. 2004;569:317–20. https://doi.org/10.1016/j.febslet.2004.06.016.

27. Thomas L, Marondedze C, Ederli L, Pasqualini S, Gehring C. Proteomic signatures implicate cAMP in light and temperature responses in Arabidopsis thaliana. Journal of Proteomics. 2013;83:47–59. https://doi.org/10.1016/j.jprot.2013.02.032.

28. Alqurashi M, Gehring C, Marondedze C. Changes in the Arabidopsis thaliana proteome implicate cAMP in biotic and abiotic stress responses and changes in energy metabolism. International Journal of Molecular Sciences. 2016;17:1–11. https://doi.org/10.3390/ijms17060852.

29. Yang H, Zhao Y, Chen N, Liu Y, Yang S, Du H, et al. A new adenylyl cyclase, putative disease-resistance RPP13-like protein 3, participates in abscisic acid-mediated resistance to heat stress in maize. Journal of Experimental Botany. 2021;72:283–301. https://doi.org/10.1093/jxb/eraa431.

30. Zhao Y, Liu Y, Ji X, Sun J, Lv S, Yang H, et al. Physiological and proteomic analyses reveal cAMP-regulated key factors in maize root tolerance to heat stress. Food and Energy Security. 2021;10:1–24. https://doi.org/10.1002/fes3.309.

31. Jarratt-Barnham E, Wang L, Ning Y, Davies JM. The complex story of plant cyclic nucleotide-gated channels. International Journal of Molecular Sciences. 2021;22:1–26. https://doi.org/10.3390/ijms22020874.

32. Liang S, Sun J, Luo Y, Lv S, Chen J, Liu Y, et al. cAMP Is a Promising Regulatory Molecule for Plant Adaptation to Heat Stress. Life. 2022;12. https://doi.org/10.3390/life12060885.

33. Thirumalaikumar VP, Gorka M, Schulz K, Masclaux-Daubresse C, Sampathkumar A, Skirycz A, et al. Selective autophagy regulates heat stress memory in Arabidopsis by NBR1-mediated targeting of HSP90.1 and ROF1. Autophagy. 2021;17:2184–99. https://doi.org/10.1080/15548627.2020.1820778.

34. Königshofer H, Tromballa HW, Löppert HG. Early events in signalling high-temperature stress in tobacco BY2 cells involve alterations in membrane fluidity and enhanced hydrogen peroxide production.

Plant, Cell and Environment. 2008;31:1771–80. https://doi.org/10.1111/j.1365-3040.2008.01880.x.

35. Saha S, Li Y, Anand-Srivastava MB. Reduced levels of cyclic AMP contribute to the enhanced oxidative stress in vascular smooth muscle cells from spontaneously hypertensive ratsThis article is one of a selection of papers published in the special issue Bridging the Gap: Where Progress in Ca. Canadian Journal of Physiology and Pharmacology. 2008;86:190–8. https://doi.org/10.1139/Y08-012.

36. Peshavariya HM, Liu G-S, Chang CWT, Jiang F, Chan EC, Dusting GJ. Prostacyclin Signaling Boosts NADPH Oxidase 4 in the Endothelium Promoting Cytoprotection and Angiogenesis. Antioxidants & Redox Signaling. 2014;20:2710–25. https://doi.org/10.1089/ars.2013.5374.

37. Paradiso A, Domingo G, Blanco E, Buscaglia A, Fortunato S, Marsoni M, et al. Cyclic AMP mediates heat stress response by the control of redox homeostasis and ubiquitin-proteasome system. Plant Cell and Environment. 2020;43:2727–42. https://doi.org/10.1111/pce.13878.

38. Das K, Roychoudhury A. Reactive oxygen species (ROS) and response of antioxidants as ROS-scavengers during environmental stress in plants. Frontiers in Environmental Science. 2014;2 DEC:1–13. https://doi.org/10.3389/fenvs.2014.00053.

39. Fortunato S, Lasorella C, Dipierro N, Vita F, de Pinto MC. Redox Signaling in Plant Heat Stress Response. Antioxidants. 2023;12. https://doi.org/10.3390/antiox12030605.

40. Mittler R. ROS Are Good. Trends in Plant Science. 2017;22:11–9. https://doi.org/10.1016/j.tplants.2016.08.002.

41. Ren J, Mi Z, Stewart NA, Jackson EK. Identification and Quantification of 2′,3′-cAMP Release by the Kidney. The Journal of Pharmacology and Experimental Therapeutics. 2009;328:855–65. https://doi.org/https://doi.org/10.1124/jpet.108.146712.

42. Lin PPC, Varner JE. Cyclic nucleotide phosphodiesterase in pea seedlings. Biochimica et Biophysica Acta (BBA) - Enzymology. 1972;276:454–74. https://doi.org/10.1016/0005-2744(72)91007-8.

43. Yu D, Song W, Tan EYJ, Liu L, Cao Y, Jirschitzka J, et al. TIR domains of plant immune receptors are 2′,3′-cAMP/cGMP synthetases mediating cell death. Cell. 2022;185:2370-2386.e18. https://doi.org/10.1016/j.cell.2022.04.032.

44. Bartsch M, Gobbato E, Bednarek P, Debey S, Schultze JL, Bautor J, et al. Salicylic Acid – Independent ENHANCED DISEASE SUSCEPTIBILITY1 Signaling in Arabidopsis Immunity and Cell Death Is Regulated by the Monooxygenase FMO1 and the Nudix Hydrolase NUDT7. 2006;18 April:1038–51. https://doi.org/10.1105/tpc.105.039982.1.

45. Ge X, Li G-J, Wang S-B, Zhu H, Zhu T, Wang X, et al. AtNUDT7, a Negative Regulator of Basal Immunity in Arabidopsis, Modulates Two Distinct Defense Response Pathways and Is Involved in Maintaining Redox Homeostasis. Plant Physiology. 2007;145:204–15. https://doi.org/10.1104/pp.107.103374.

46. Kosmacz M, Luzarowski M, Kerber O, Leniak E, Gutiérrez-Beltrán E, Moreno JC, et al. Interaction of 2',3'-cAMP with Rbp47b Plays a Role in Stress Granule Formation. Plant physiology. 2018;177:411–21. https://doi.org/10.1104/pp.18.00285.

47. Luo W, Xu Y, Cao J, Guo X, Han J, Zhang Y, et al. COLD6-OSM1 module senses chilling for cold tolerance via 2′,3′-cAMP signaling in rice. Molecular Cell. 2024;84:4224-4238.e9. https://doi.org/10.1016/j.molcel.2024.09.031.

48. Lefkimmiatis K, Moyer MP, Curci S, Hofer AM. "cAMP sponge": A buffer for cyclic adenosine 3′, 59-monophosphate. PLoS ONE. 2009;4:2–9. https://doi.org/10.1371/journal.pone.0007649.

49. Dündar G, Ramirez VE, Poppenberger B. The heat shock response in plants: new insights into modes of perception, signaling, and the contribution of hormones. Journal of Experimental Botany. 2025;76:1970–7. https://doi.org/10.1093/jxb/erae419.

50. Chaffai R, Ganesan M, Cherif A. Mechanisms of Plant Response to Heat Stress: Recent Insights BT - Plant Adaptation to Abiotic Stress: From Signaling Pathways and Microbiomes to Molecular

Mechanisms. In: Chaffai R, Ganesan M, Cherif A, editors. Singapore: Springer Nature Singapore; 2024. p. 83–105. https://doi.org/10.1007/978-981-97-0672-3_5.

51. Bourgine B, Guihur A. Heat Shock Signaling in Land Plants: From Plasma Membrane Sensing to the Transcription of Small Heat Shock Proteins. Frontiers in Plant Science. 2021;12 August:1–10. https://doi.org/10.3389/fpls.2021.710801.

52. Distéfano AM, Bauer V, Cascallares M, López GA, Fiol DF, Zabaleta E, et al. Heat stress in plants: Sensing, signalling, and ferroptosis. Journal of Experimental Botany. 2025;76:1357–69. https://doi.org/10.1093/jxb/erae296.

53. Miller G, Schlauch K, Tam R, Cortes D, Torres MA, Shulaev V, et al. The Plant NADPH Oxidase RBOHD Mediates Rapid Systemic Signaling in Response to Diverse Stimuli. Science Signaling. 2009;2:ra45–ra45. https://doi.org/10.1126/scisignal.2000448.

54. Driedonks N, Xu J, Peters JL, Park S, Rieu I. Multi-level interactions between heat shock factors, heat shock proteins, and the redox system regulate acclimation to heat. Frontiers in Plant Science. 2015;6 NOVEMBER:1–9. https://doi.org/10.3389/fpls.2015.00999.

55. Domingo G, Marsoni M, Davide E, Fortunato S, de Pinto MC, Bracale M, et al. The cAMP-dependent phosphorylation footprint in response to heat stress. Plant Cell Reports. 2024;43:1–14. https://doi.org/10.1007/s00299-024-03213-y.

56. Zhang J, Kirkham MB. Antioxidant responses to drought in sunflower and sorghum seedlings. New Phytologist. 1996;132:361–73. https://doi.org/10.1111/j.1469-8137.1996.tb01856.x.

57. Lichtenthaler HKBT-M in E. [34] Chlorophylls and carotenoids: Pigments of photosynthetic biomembranes. In: Plant Cell Membranes. Academic Press; 1987. p. 350–82. https://doi.org/https://doi.org/10.1016/0076-6879(87)48036-1.

58. Kaundal A, Rojas CM, Mysore KS. Measurement of NADPH Oxidase Activity in Plants. Bio-protocol. 2012;2:e278. https://doi.org/10.21769/BioProtoc.278.

59. Kruger NJ. The Bradford method for protein quantitation. The protein protocols handbook. 2009;:17–24.

60. Jiang M, Zhang J. Involvement of plasma-membrane NADPH oxidase in abscisic acid- and water stress-induced antioxidant defense in leaves of maize seedlings. Planta. 2002;215:1022–30. https://doi.org/10.1007/s00425-002-0829-y.

61. Middleton AJ, Vanderbeld B, Bredow M, Tomalty H, Davies PL, Walker VK. Plant Cold Acclimation. 2014;1166:255–77. https://doi.org/10.1007/978-1-4939-0844-8.

62. Robinson MD, McCarthy DJ, Smyth GK. edgeR: A Bioconductor package for differential expression analysis of digital gene expression data. Bioinformatics. 2009;26:139–40. https://doi.org/10.1093/bioinformatics/btp616.

63. Wickham H. Data Analysis BT - ggplot2: Elegant Graphics for Data Analysis. In: Wickham H, editor. Cham: Springer International Publishing; 2016. p. 189–201. https://doi.org/10.1007/978-3-319-24277-4_9.

64. Etoh K, Nakao M. A web-based integrative transcriptome analysis, RNAseqChef, uncovers the cell/tissue type-dependent action of sulforaphane. Journal of Biological Chemistry. 2023;299:104810. https://doi.org/10.1016/j.jbc.2023.104810.

65. Taylor SC, Nadeau K, Abbasi M, Lachance C, Nguyen M, Fenrich J. The Ultimate qPCR Experiment: Producing Publication Quality, Reproducible Data the First Time. Trends in Biotechnology. 2019;37:761–74. https://doi.org/10.1016/j.tibtech.2018.12.002.

66. Lasorella C, Fortunato S, Dipierro N, Jeran N, Tadini L, Vita F, et al. Chloroplast-localized GUN1 contributes to the acquisition of basal thermotolerance in Arabidopsis thaliana. Frontiers in Plant Science. 2022;13 December:1–14. https://doi.org/10.3389/fpls.2022.1058831.

67. Ge SX, Jung D, Jung D, Yao R. ShinyGO: A graphical gene-set enrichment tool for animals and plants. Bioinformatics. 2020;36:2628–9. https://doi.org/10.1093/bioinformatics/btz931.

68. Zhao J, Guo Y, Fujita K, Sakai K. Involvement of cAMP signaling in elicitor-induced phytoalexin accumulation in Cupressus lusitanica cell cultures. New Phytologist. 2004;161:723–33. https://doi.org/10.1111/j.1469-8137.2004.00976.x.

69. Ma W, Qi Z, Smigel A, Walker RK, Verma R, Berkowitz GA. Ca2+, cAMP, and transduction of non-self perception during plant immune responses. Proceedings of the National Academy of Sciences of the United States of America. 2009;106:20995–1000. https://doi.org/10.1073/pnas.0905831106.

70. Jiang J, Fan LW, Wu WH. Evidences for involvement of endogenous cAMP in Arabidopsis defense responses to Verticillium toxins. Cell Research. 2005;15:585–92. https://doi.org/10.1038/sj.cr.7290328.

71. Haider S, Iqbal J, Naseer S, Yaseen T, Shaukat M, Bibi H, et al. Molecular mechanisms of plant tolerance to heat stress: current landscape and future perspectives. Plant Cell Reports. 2021;40:2247–71. https://doi.org/10.1007/s00299-021-02696-3.

72. Rizhsky L, Liang H, Mittler R. The Combined Effect of Drought Stress and Heat Shock on Gene Expression in Tobacco. Plant Physiology. 2002;130:1143–51. https://doi.org/10.1104/pp.006858.

73. Camejo D, Torres W, Nuñez M. Effect of salinity on the initial stages of development in two cultivars of tomato (Lycopersicon esculentum Mill). Proceedings of the Interamerican Society for Tropical Horticulture. 2001;43 PP-Homestead:1–5.

74. Mathur S, Agrawal D, Jajoo A. Photosynthesis: Response to high temperature stress. Journal of Photochemistry and Photobiology B: Biology. 2014;137:116–26. https://doi.org/10.1016/j.jphotobiol.2014.01.010.

75. Gounaris K, Brain APR, Quinn PJ, Williams WP. Structural and functional changes associated with heat-induced phase-separations of non-bilayer lipids in chloroplast thylakoid membranes. FEBS Letters. 1983;153:47–52. https://doi.org/10.1016/0014-5793(83)80117-3.

76. Babbar R, Karpinska B, Grover A, Foyer CH. Heat-Induced Oxidation of the Nuclei and Cytosol. Frontiers in Plant Science. 2021;11 January:1–16. https://doi.org/10.3389/fpls.2020.617779.

77. Xu R, Guo Y, Peng S, Liu J, Li P, Jia W, et al. Molecular targets and biological functions of camp signaling in arabidopsis. Biomolecules. 2021;11:1–35. https://doi.org/10.3390/biom11050688.

78. Lu C, Li W, Feng X, Chen J, Hu S, Tan Y, et al. The Dynamic Remodeling of Plant Cell Wall in Response to Heat Stress. Genes. 2025;16:1–15. https://doi.org/10.3390/genes16060628.

79. Yu F, Qian L, Nibau C, Duan Q, Kita D, Levasseur K, et al. FERONIA receptor kinase pathway suppresses abscisic acid signaling in Arabidopsis by activating ABI2 phosphatase. Proceedings of the National Academy of Sciences. 2012;109:14693–8. https://doi.org/10.1073/pnas.1212547109.

80. Wang K, He J, Zhao Y, Wu T, Zhou X, Ding Y, et al. EAR1 Negatively Regulates ABA Signaling by Enhancing 2C Protein Phosphatase Activity. The Plant Cell. 2018;30:815–34. https://doi.org/10.1105/tpc.17.00875.

81. Li T, Jia W, Peng S, Guo Y, Liu J, Zhang X, et al. Endogenous cAMP elevation in Brassica napus causes changes in phytohormone levels. Plant Signaling and Behavior. 2024;19:1–15. https://doi.org/10.1080/15592324.2024.2310963.

82. Chen ST, He NY, Chen JH, Guo FQ. Identification of core subunits of photosystem II as action sites of HSP21, which is activated by the GUN5-mediated retrograde pathway in Arabidopsis. Plant Journal. 2017;89:1106–18. https://doi.org/10.1111/tpj.13447.

83. John S, Apelt F, Kumar A, Acosta IF, Bents D, Annunziata MG, et al. The transcription factor HSFA7b controls thermomemory at the shoot apical meristem by regulating ethylene biosynthesis and signaling in Arabidopsis. Plant Communications. 2024;5:100743. https://doi.org/10.1016/j.xplc.2023.100743.

84. Sweetman C, Waterman CD, Rainbird BM, Smith PMC, Jenkins CD, Day DA, et al. Atndb2 is the main external NADH dehydrogenase in mitochondria and is important for tolerance to environmental stress. Plant Physiology. 2019;181:774–88. https://doi.org/10.1104/pp.19.00877.

85. Zhang Y, Song R-F, Hu X-Y, Zhou H, Wang W, Zhang J, et al. Arabidopsis HSFA1b functions as a heat sensor inhibiting OST1-mediated stomatal closure through its adenylate-cyclase activity. Molecular Plant. 2025;1:1549–66. https://doi.org/10.1016/j.molp.2025.07.018.

Chapter 5: General conclusions

This PhD research highlights the unique yet interconnected roles of the two cAMP isomers, 3',5'-cAMP and 2',3'-cAMP, in Arabidopsis thaliana. The findings indicate that 3',5'-cAMP, synthesized by adenylate cyclases, functions as a precise and dynamic modulator of cellular organization and biogenesis, regulating specific protein targets such as the CNGC2 and CNGC18 ion channels. In contrast, 2',3'-cAMP, generated as a byproduct of RNA degradation, appears to exert broader, system-level effects, particularly on transcriptional regulation. Notably, both isomers attenuate H_2O_2-induced oxidative stress and mitigate ion flux imbalances under stress, although they likely do so through distinct mechanisms.

The results further emphasize the central significance of 3',5'-cAMP in the heat stress response of plants. Arabidopsis lines with buffered 3',5'-cAMP levels exhibited heightened sensitivity to heat, manifesting as reduced growth, impaired photosynthesis, and altered chloroplast structure. This vulnerability was associated with persistent redox imbalance and a diminished antioxidant response during recovery. Collectively, these observations support the role of 3',5'-cAMP as a crucial coordinator of protective mechanisms that mediate plant resilience in stressful environments.

Overall, these findings underscore the importance of investigating both the specific functions and potential interactions between 3',5'-cAMP and 2',3'-cAMP in plant biology. Recognizing their complementary and possibly cooperative activities opens new perspectives on how cyclic nucleotides may jointly contribute to the orchestration of stress response networks. While further studies are necessary to elucidate these relationships fully, this work establishes an essential foundation for future research aimed at clarifying the complexity and broader impact of cAMP signaling in plant adaptation and resilience.

Appendices

Supplementary materials (chapter 3 and chapter 4) are available in the link below:

https://drive.google.com/drive/folders/1tnrC4SqqbhsRM4RNCJkCkhLlSYBPfDT-?usp=drive_link

Figure S1. PCA plot

Figure S2. Venn diagram – comparison with Xu et al., 2021

Table S1. qPCR primers

Table S2- S11. Clusters and ShinyGO enrichment

cAMP sponge expression:

WT plants and cAS plants (1 and 3 lines) were grown at 22 °C for 14 days under a 16/8 h light/dark regime. The presence and expression of the cAMP sponge were confirmed *in vivo* through the detection of fluorescence of mCherry, which is fused to the sponge. The presence of the sponge protein cAMP was detected by mCherry fluorescence. They were visualized using an Olympus IX51 inverted fluorescence microscope (Olympus, Tokyo, Japan). The rhodopsin filter, which has an absorption peak at 585 nm and an emission peak at 610 nm, was used to visualize mCherry. It is confirmed in both cAS lines (cAS1 and cAS3), as shown by mCherry-associated fluorescence in the roots (Fig. 20D) and leaves (Fig. 20B). In accordance with the use of a constitutive promoter, the mCherry fluorescence was uniformly distributed in cAS seedlings, i.e. cotyledon leaves, hypocotyl and roots [1]. As expected, the roots of the WT plants do not show any fluorescence signal (Fig. 20C). The leaves of WT plants (Fig. 20A) display an autofluorescence signal due to chlorophylls and secondary metabolites.

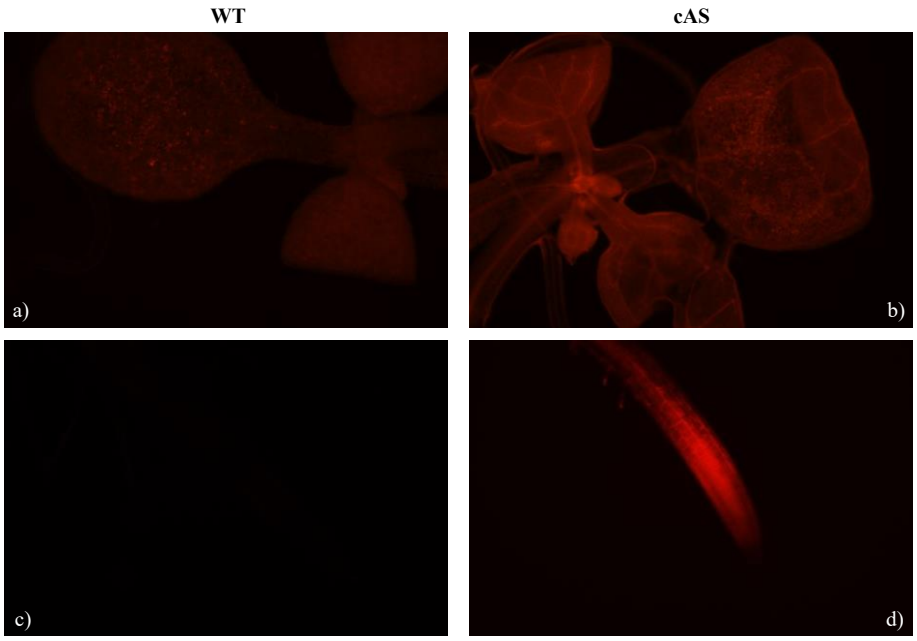

Fig.20 Visualization of mCherry fluorescence in the cAMP sponge protein in WT (a) and cAS leaves (b), and in WT (c) and cAS roots (d). Leaves photos were acquired at 4X; roots photos were acquired at 10X.

References:

1. Sabetta W, Vandelle E, Locato V, Costa A, Cimini S, Bittencourt Moura A, et al. Genetic buffering of cyclic AMP in Arabidopsis thaliana compromises the plant immune response triggered by an avirulent strain of Pseudomonas syringae pv. tomato. Plant Journal. 2019;98:590–606. https://doi.org/10.1111/tpj.14275.

Published papers during the PhD with contribution from the candidate:

- Domingo, G., Marsoni, M., Davide, E. *et al.* The cAMP-dependent phosphorylation footprint in response to heat stress. *Plant Cell Rep* 43, 137 (2024). https://doi.org/10.1007/s00299-024-03213-y
- Fortunato S., Domingo G., Davide E., Lasorella C., Bracale M., Vannini C., de Pinto M.C., Dual function plant cryptic nucleotide cyclases, Chapter 7 in Foundations and Frontiers in Enzymology, Cryptic Enzymes and Moonlighting Proteins, Editor(s): Helen Irving, Chris Gehring, Aloysius Wong, Academic Press, 2025, Pages 135-172, ISBN 9780443157196, https://doi.org/10.1016/B978-0-443-15719-6.00007-6.
- Vaccarella O.M., Giove S., Davide E., Dipierro N., Vannini C., Marsoni M., Domingo G., Fortunato S., Marcotuli I., Gadaleta A., de Pinto M.C., Vita V. Physiological response to phosphate fertilization in Durum wheat (under revision)

Acknowledgement

Scientific support from CRIETT center of University of Insubria (instrument code MIC01) is greatly acknowledged.

RNA-Seq was performed by Novogene (https://www.novogene.com).